Department of Aerospace Engineering

# AIAA Individual Aircraft Design Proposal

# The Renosaur

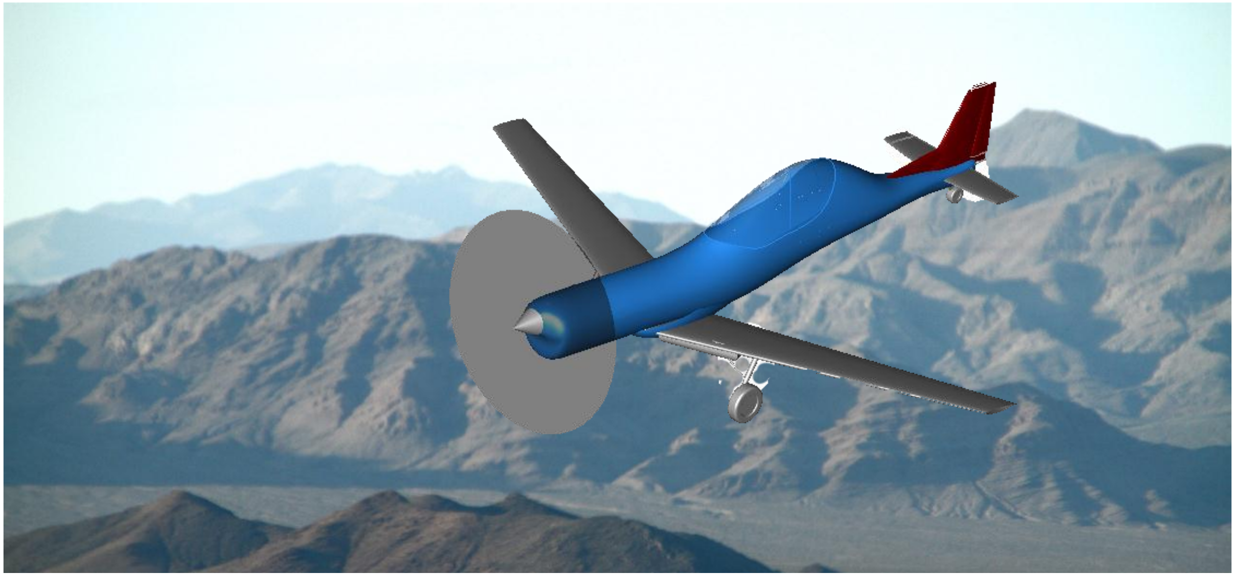

*Author:*
Jorrit Vervoordeldonk

*Faculty and Project Advisors:*
University of Kansas: Dr. Ron Barrett
Delft University of Technology: Prof. Roelof Vos

June 9, 2012

# AIAA Individual Aircraft Design Proposal

# The Renosaur

Designer: Mr. Jorrit Vervoordeldonk

AIAA Member ID: 446077

Email: jorrit.vervoordeldonk@gmail.com

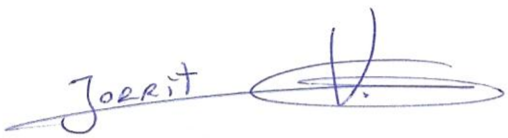

8 June 2012

Signature of Designer | Date

Faculty/ Project Advisor (University of Kansas): Dr. Ron Barrett

AIAA Member ID: 022393

Email: adaptivebarrett@yahoo.com

 

1 Dec. 2011

Signature of Faculty Advisor | Signature of Project Advisor | Date

Faculty/Project Advisor (Delft University of Technology): Prof. Roelof Vos

AIAA Member ID: 254874

Email: r.vos@tudelft.nl

 

7 June 2012

Signature of Faculty Advisor | Signature of Project Advisor | Date

## Acknowledgments

The design of this aircraft could not have been completed without the contribution and enthusiasm of many individuals who guided me through the aircraft design process. First, the author would like to thank and acknowledge Dr. Ron Barrett for his guidance and advice during the time spent working on the design at the University of Kansas. Without his insights and enthusiasm the author would not have been able to accomplish the design to the level it is today. Furthermore, the author would like to thank Dr. Perry Rea (Chief Engineer, New Small Airplane Product Development at Boeing Commercial Airplanes) for his comments and advice on the design philosophy of the Renosaur. Finally, honor should be paid to Prof. Roelof Vos, the faculty advisor at Delft University of Technology. He helped me to improve the design during the final months of the project.


**Figure 1: P-51D Mustang at the Air and Space Museum in Washington DC**

# TABLE OF CONTENTS

Page #

Acknowledgments ..... iii
List of Symbols ..... vi
Judging Assistance Page ..... 1
1 VALIDATION DATASET, METHOD CALIBRATION AND INTRODUCTION ..... 2
1.1 BACKGROUND ..... 2
1.2 RACE TRACK ANALYSIS ..... 3
1.3 MISSION SPECIFICATION AND PROFILE ..... 5
1.3.1 MISSION SPECIFICATION ..... 5
1.3.2 MISSION PROFILE ..... 5
1.4 DESIGN METHOD AND COMPUTATIONAL PROGRAMS ..... 6
1.5 RENOSAUR DESIGN PHILOSOPHY ..... 8
1.6 SAFETY MEASURES ..... 8
2 DESIGN JUSTIFICATION AND TECHNICAL APPROACH TO MEET MISSION REQUIREMENTS ..... 9
2.1 WING AND POWER LOADING ..... 9
2.2 DESIGN SPACE SWEEP ..... 10
3 CLASS I & II SIZING METHODS AND SENSITIVITIES ..... 14
3.1 DESCRIPTION OF SIMILAR AIRPLANES ..... 14
3.2 MISSION WEIGHTS ..... 17
3.3 WEIGHT SENSITIVITIES ..... 19
3.4 SIZING PLOT ..... 21
4 THREE-VIEW OF THE GENERAL ARRANGEMENT AND SALIENT CHARACTERISTICS ..... 22
5 INBOARD PROFILE AND CLASS II DESIGN ..... 25
5.1 OVERALL CONFIGURATION ..... 25
5.2 FUSELAGE CONFIGURATION ..... 25
5.3 ENGINE CONFIGURATION ..... 25
5.4 WING CONFIGURATION ..... 26
5.5 EMPENNAGE CONFIGURATION ..... 27
5.6 LANDING GEAR CONFIGURATION ..... 28
6 CLASS II WEIGHT AND BALANCE ..... 30
6.1 CLASS II WEIGHT AND BALANCE CALCULATIONS ..... 30
6.2 CLASS II CG POSITIONS ON THE AIRFRAME, CG EXCURSION ..... 32
7 CLASS II DRAG BUILD-UPS & DRAG POLARS ..... 35
7.1 CLASS II DRAG POLARS ..... 35
7.1.1 WETTED AREA DETERMINATION ..... 35
7.1.2 DRAG POLAR ANALYSIS ..... 36
7.2 IMPACT OF L/D ANALYSIS ON DESIGN ..... 37
7.3 CLASS II DRAG BUILD-UPS & DRAG POLARS ..... 38
8 CLASS II PROPULSION PERFORMANCE ..... 39
8.1 ENGINE SPECIFICATIONS ..... 39
8.2 ENGINE PERFORMANCE AND MATERIALS ..... 39
8.3 ENGINE SELECTION RISKS ..... 40
9 CLASS II STABILITY AND CONTROL ..... 41
9.1 STATIC LONGITUDINAL STABILITY ..... 41
9.2 STATIC DIRECTIONAL STABILITY ..... 42

9.3 CLASS II STABILITY & CONTROL ....................44
10 STRUCTURES .................... 48
10.1 LAYOUT OF STRUCTURAL COMPONENTS ....................48
10.1.1 Fuselage ....................48
10.1.2 Wing ....................48
10.1.3 Empennage ....................48
10.1.4 Landing Gear Integration ....................49
10.2 CAD DRAWINGS OF STRUCTURAL LAYOUT ....................49
11 SYSTEMS .................... 51
11.1 DESCRIPTION OF THE FLIGHT CONTROL SYSTEM ....................51
11.1.1 Ailerons ....................52
11.1.2 Elevator ....................53
11.1.3 Rudder ....................54
11.1.4 Trim Controls ....................54
11.1.5 Power Controls ....................55
11.2 DESCRIPTION OF THE FUEL SYSTEM ....................55
11.3 DESCRIPTION OF THE ELECTRICAL SYSTEM ....................57
11.4 DESCRIPTION OF THE HYDRAULIC SYSTEM ....................58
11.5 CONFLICT ANALYSIS ....................59
12 ADVANCED TECHNOLOGIES .................... 60
12.1 ADVANCED TECHNOLOGIES USED ....................60
12.1.1 Fly-by-wire flight control system ....................60
12.1.2 Formula One engines ....................60
12.1.3 Advanced materials ....................60
13 COST ESTIMATION .................... 61
13.1 COST PHILOSOPHY ....................61
13.2 COST ESCALATION FACTOR ....................62
13.3 AMPR WEIGHT ....................62
13.4 RDTE COST ....................63
13.5 ACQUISITION COST ....................64
13.6 OPERATING COST ....................65
13.7 LIFE CYCLE COST AND DISPOSAL COST ....................66
14 REFERENCES .................... 67

## List of Symbols

| Symbol | Description | Units |
|---|---|---|
| $A$ | Aspect Ratio | (~) |
| $A$ | Regression Constant | (~) |
| $B$ | Regression Constant | (~) |
| $c$ | Chord | (ft) |
| $\bar{c}$ | Mean Geometric Chord | (ft) |
| $c_f$ | Skin Friction Coefficient | (~) |
| $c_p$ | Specific Fuel Consumption | (lbf/hp-hr) |
| $C$ | Cost | ($) |
| $C_L$ | Lift Coefficient | (~) |
| $C_D$ | Drag Coefficient | (~) |
| $C_{D_0}$ | Zero Lift Drag Coefficient | (~) |
| $C_{N_\beta}$ | Yawing Moment Coefficient due to Sideslip | (1/deg) |
| $d_f$ | Fuselage Diameter | (in) |
| $D_0$ | Tire Diameter | (in) |
| $e$ | Oswald's Efficiency Factor | (~) |
| $E$ | Endurance | (hr) |
| $f$ | Parasite area | ($ft^2$) |
| $F_c$ | Required Control Force | (lbf) |
| $i$ | Incidence Angle | (deg) |
| $I$ | Moment of Inertia | ($ft^4$) |
| $l$ | Length | (in) |
| $L/D$ | Lift-to-Drag Ratio | (~) |
| $M_{DD}$ | Mach Drag Divergence Number | (~) |
| $M_{ff}$ | Mission Fuel Fraction | (~) |
| $n$ | Load Factor | (g) |
| $P$ | Power | (hp) |
| $R$ | Range | (mi) |
| $S$ | Wing Area | ($ft^2$) |
| $t/c$ | Thickness ratio | (~) |
| $V$ | Velocity | (knots, ft/s) |

## List of Symbols (Continued)

| Symbol | Description | Units |
|---|---|---|
| $W$ | Weight | (lbf) |

| Greek Symbol | Description | Units |
|---|---|---|
| $\Gamma$ | Dihedral Angle | (deg) |
| $\eta$ | Spanwise Station, Fraction of Span | (~) |
| $\eta_p$ | Propulsive Efficiency | (~) |
| $\theta_{fc}$ | Fuselage Cone Angle | (deg) |
| $\lambda$ | Taper ratio | (~) |
| $\Lambda_{c/4}$ | Quarter Chord Sweep Angle | (deg) |

| Subscript | Description |
|---|---|
| $aft$ | Aft |
| $cg$ | Center of Gravity |
| $clean$ | Clean wing |
| $crew$ | Crew |
| $e$ | Elevator |
| $E$ | Empty |
| $f$ | Fuselage |
| $fc$ | Fuselage Cone |
| $fwd$ | Forward |
| $F$ | Fuel |
| $h$ | Horizontal Wing |
| $i$ | Inboard |
| $L$ | Landing |
| $m$ | Main Gear |
| $max$ | Maximum |
| $mgc$ | Mean Geometric Chord |
| $o$ | Outboard |
| $oe$ | Operating Empty |

## List of Symbols (Continued)

| Subscript | Description |
|---|---|
| $PL$ | Payload |
| $r$ | Rudder |
| $t$ | Tip |
| $t$ | Tail Gear |
| $TO$ | Takeoff |
| $v$ | Vertical Wing |
| $w$ | Wing |
| $wet$ | Wetted |

| Abbreviation | Description |
|---|---|
| AAA | Advanced Aircraft Analysis |
| AGL | Above Ground Level |
| AIAA | American Institute of Aeronautics and Astronautics |
| AMPR | Aeronautical Manufacturers Planning Report |
| BL | Buttock Line |
| c.g. | Center of Gravity |
| CEF | Cost Escalation Factor |
| CPI | Consumer Price Index |
| FS | Fuselage Station |
| MSL | Mean Sea Level |
| RDTE | Research, Development, Test and Evaluation |
| RFP | Request for Proposal |
| WL | Water Line |

## Judging Assistance Page

| Basis for Judging | Points |
|---|---|
| 1. Technical Content (35 points) | |
| 2. Organization and Presentation (20 points) | |
| 3. Originality (20 points) | |
| 4. Practical Application and Feasibility (25 points) | |

| **The technical proposal must convincingly demonstrate that the analysis methodology is realistic and that the design that results from it satisfies the requirements. The proposal should satisfy the following tasks to show how the design would be developed.** | **Presented in section:** |
|---|---|
| 1. Present the validation dataset collected, show how it was used, and explain any method calibration performed. | 1 |
| 2. Justify the final design, and describe the technologies and technical approach used to meet the mission requirements. | 2 |
| 3. Provide sizing plots used to guide the design selection. Describe sensitivity studies. | 3 |
| 4. Include a dimensioned 3-view general arrangement drawing. | 4 |
| 5. Include an inboard profile showing the internal arrangement. | 5 |
| 6. Show a weight breakdown of the major components and systems. Show weight and CG envelope to cover the following loadings:<br>a. Race b. Ferry c. Takeoff d. Landing | 6 |
| 7. Show estimated component drag build-ups (parasite) and drag polars (+ lift dependent profile, induced, and trim) for all conditions. Remember to account for compressibility and cooling drag. | 7 |
| 8. Show estimated propulsion performance including engine power, fuel flow, and propulsive efficiency for all conditions. Remember to account for compressibility. | 8 |
| 9. Show estimated stability for all flight and loading conditions. The pilot's force required to attain the maximum of 6g load must be reasonable, but not so light that the aircraft is easily over controlled. For stick controls, this force must be between 15 and 35 lbs. | 9 |
| 10. Include an illustrated description of the primary load bearing airframe structure, and state rationale for material selection. | 10 |
| 11. Include descriptions of the major aircraft systems. | 11 |
| 12. Describe any advanced technologies or design approaches and their relative benefits as used to obtain performance improvements. Address risk mitigation if these technologies fail to materialize, including cost increase and performance decrements. | 12 |
| 13. Provide flyaway cost estimate for production run of 1 and 10 units. Provide fixed and hourly cost estimates. | 13 |

# 1 VALIDATION DATASET, METHOD CALIBRATION AND INTRODUCTION

This section introduces the design challenge, as set in the Request for Proposal (RFP) of the American Institute of Aeronautics and Astronautics (AIAA) Undergraduate Individual Aircraft Design Competition (Ref. 1). First, the background, the race and the race course of the National Air Races are presented. Next, the overall aircraft is introduced along with the validation dataset and the method calibration. Special attention is given to public safety during the race. Finally, any computer programs and codes used in the design process are introduced as well.

## 1.1 BACKGROUND

The National Championship Air Races are held every year in September at Reno Stead Airport, Nevada. Over a span of five days, six classes of aircraft are raced, culminating in the popular Unlimited Class. This class has been dominated for decades by modified examples of classic piston-engined, propeller-driven fighters. The few competitive aircraft have been extensively modified and appear to have reached the zenith of what may be achievable using this approach. There have been few examples of specially-designed Unlimited Class air racers, but they have not proven competitive. In order to reinvigorate this sport, new clean-sheet designs are needed that are competitive with the best current racers (Ref. 1).

The Unlimited Class Race is open to piston-powered aircraft with an empty weight over 4,500 lbf. The last decades this class has been dominated by modified World War II aircraft, like the P-51 Mustang and the F8F Bearcat. The winners of the Unlimited Class in the period 2007 - 2009 are presented in Table 1.1. The current speed record in is set in 2003 by ‘Dago Red’, a modified P-51D Mustang, to be 507 mph (Ref. 2). The aircraft fly a qualifying round, after which the fastest aircraft proceed to the Unlimited Gold Heats. Finally, the Unlimited Breitling Gold Race, consisting of 8 laps, decides on the winner of the Unlimited Class Air Races. The Unlimited Breitling Gold Race track is 66.99 miles long.

**Table 1.1: Winners Unlimited Class Air Race Gold Race (Ref. 2)**

| Year | Winners | Aircraft | Top speed (*mph*) |
|---|---|---|---|
| 2007 | 1st – Rare bear<br>2nd – Czech Mate<br>3rd – Spirit of Texas | F8F-2 Bearcat<br>Yak-11<br>FB II Sea Fury | 478<br>434<br>432 |
| 2008 | 1st – Strega<br>2nd – Dago Red<br>3rd – September Fury | P-51D Mustang<br>P-51D Mustang<br>FB II Sea Fury | 483<br>474<br>473 |
| 2009 | 1st – Strega<br>2nd – Rare Bear<br>3rd – Czech Mate | P-51D Mustang<br>F8F-2 Bearcat<br>Yak-11 | 491<br>479<br>464 |

## 1.2 RACE TRACK ANALYSIS

The aircraft fly around the Unlimited Course, an oval race track which is 8.43 miles long, presented in Figure 1.1. To determine the maximum number of g's pulled in a turn, the race track is analyzed using the optimum race path presented in Figure 1.2 (Ref. 3). The minimum turn radius will be determined by pylon 5, since around this pylon the aircraft have to change their flight direction the most: 53 degrees. The distance between pylon 4 and 5 and pylon 5 and 6 is equal; the minimum turning radius is therefore determined by the circle through pylon 4, 5 and 6. The radius of this circle, and thus the minimum turn radius is determined to be 5180 feet. Equation 1.1 is used to determine the maximum number of g's pulled in a turn. Assuming a flight speed of 600 mph, as explained in Section 2.1, the maximum number of g's pulled is determined to be 3.5.

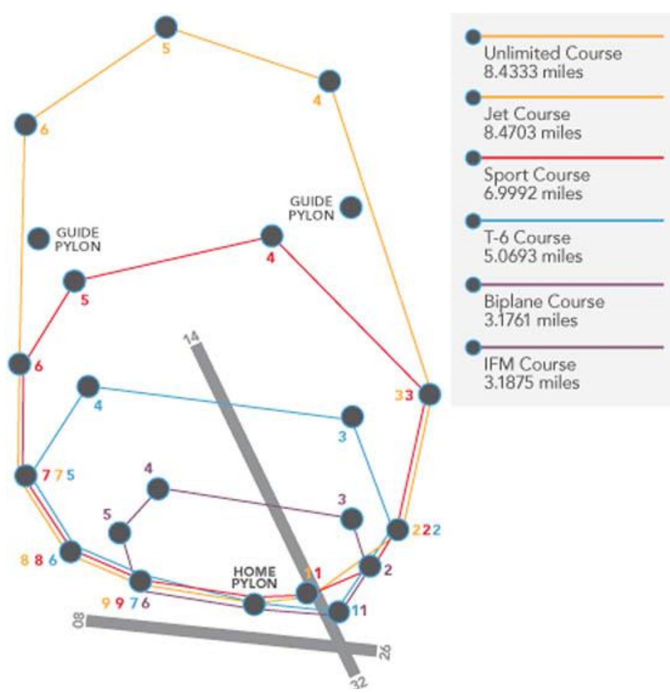


**Figure 2.1: Unlimited Course**

$$R = \frac{V^2}{g\sqrt{n^2-1}}$$ (Equation 1.1)

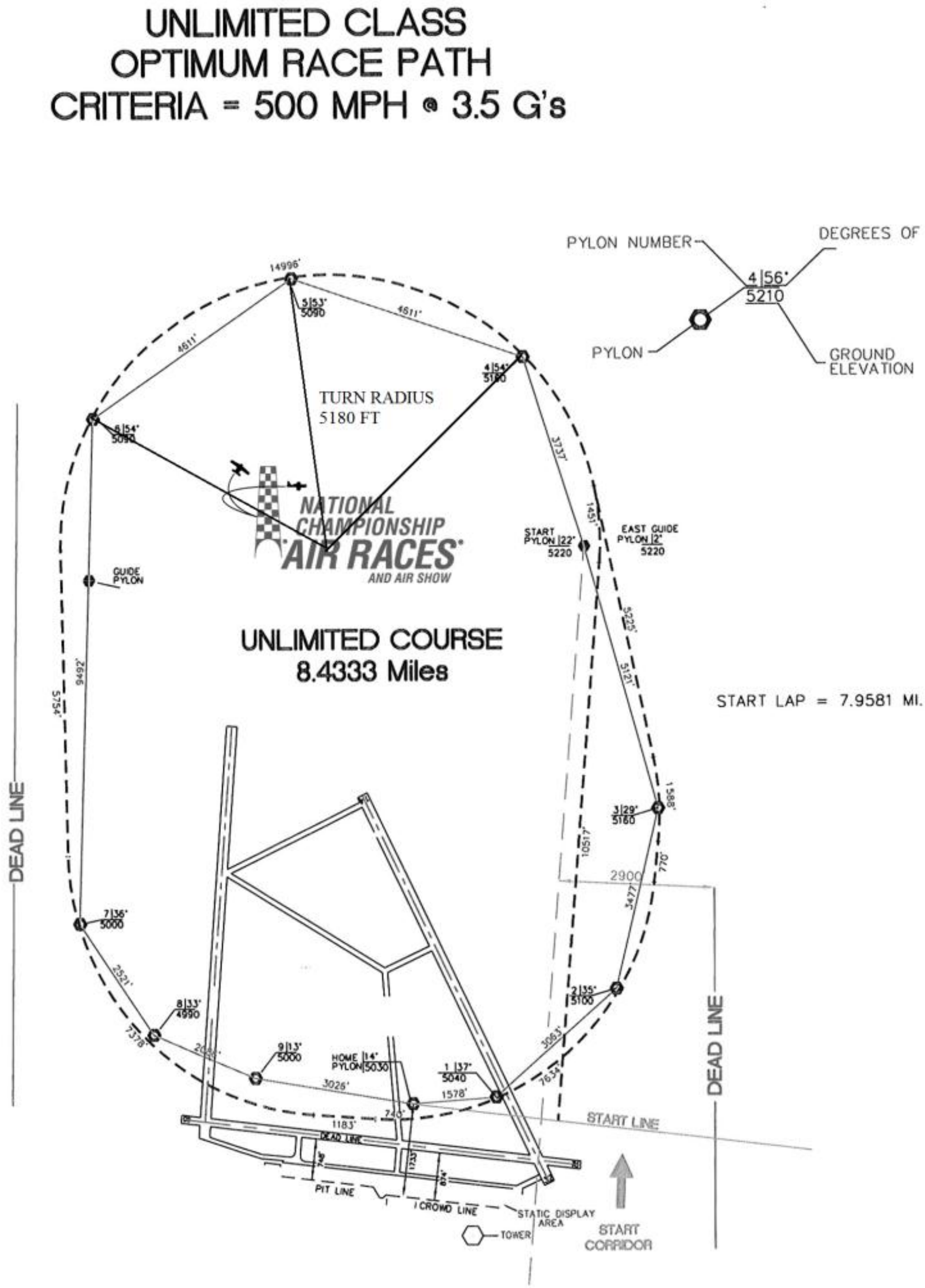


**Figure 3.2: Turn Radius Determination (Ref. 3)**

## 1.3 MISSION SPECIFICATION AND PROFILE

### 1.3.1 MISSION SPECIFICATION

The mission specification for the Renosaur is given by the AIAA. The Unlimited Class requires the designed aircraft to be piston-driven with an empty weight greater than 4,500 pounds and capable of pulling 6 g's. Furthermore, the following miscellaneous specifications are provided (Ref. 1):

- FAA experimental certification basis
- Takeoff and landing performance appropriate for Stead Airfield, with consideration of engine-out emergency operation
- Pilot visibility should be appropriate for safe race operations
- Ferry capability of 500 nautical miles

The AIAA specifies that all performance will be computed at representative race day atmospheric conditions except for the ferry cruise, which is at standard atmospheric conditions. The conditions under which the race takes place are specified in the RFP. The conditions at Reno Stead Airport during the races are specified as following (Ref. 1):

- Races held during 14-18 September
- Altitude of 5,100 ft MSL (50 ft AGL)
- Temperature of 78$^{o}$ F and a pressure of 29.95 in

### 1.3.2 MISSION PROFILE

The Renosaur must be able to fly two mission profiles: the ferry mission and the race mission. The ferry mission is necessary to fly to and from the Reno races; the race mission is the Unlimited Class Race itself. The mission profiles for the ferry and race mission are given in Figure 1.3 and Figure 1.4, respectively.

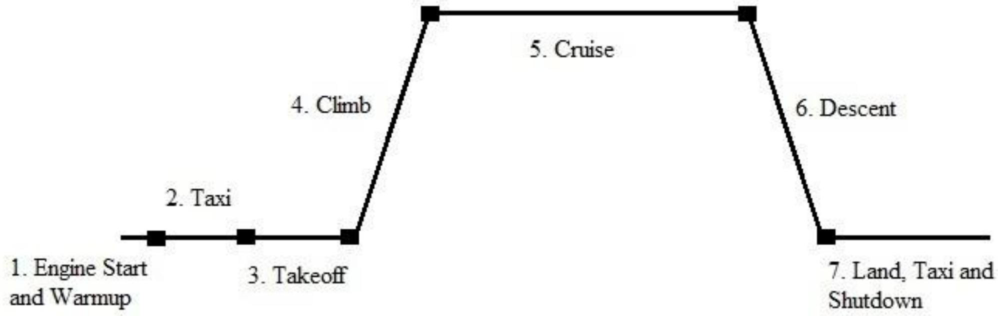


**Figure 1.3: Ferry mission profile**

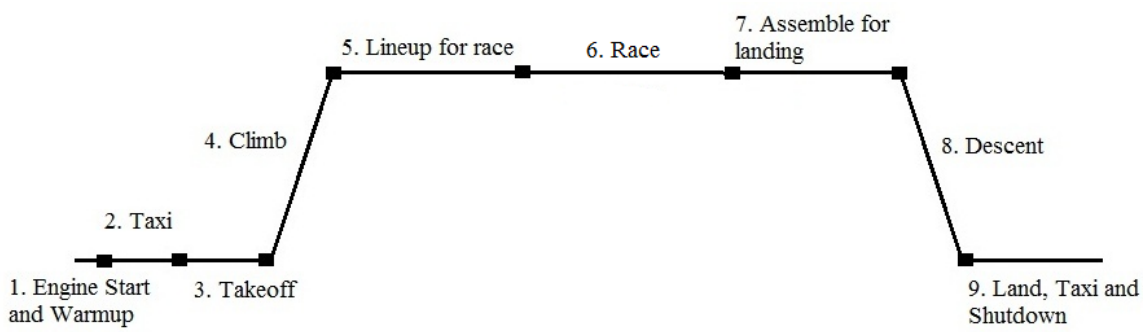


**Figure 1.4: Race mission profile**

## 1.4 DESIGN METHOD AND COMPUTATIONAL PROGRAMS

The method followed in the preliminary design of the Renosaur is the Airplane Design method by Dr. Jan Roskam (Ref. 4-9). The preliminary design sequence described in this method is followed and additional methods are used where considered necessary. The design sequence is presented in Figure 1.5. Furthermore, a number of computer programs and codes are used in the design process of the Renosaur. Most of the technical work is performed in MS Excel and the Advanced Aircraft Analysis (AAA) program (Ref. 10). Values are computed where possible both in Excel and AAA and the results are compared. The CAD drawings are produced in the CATIA (Ref. 11).

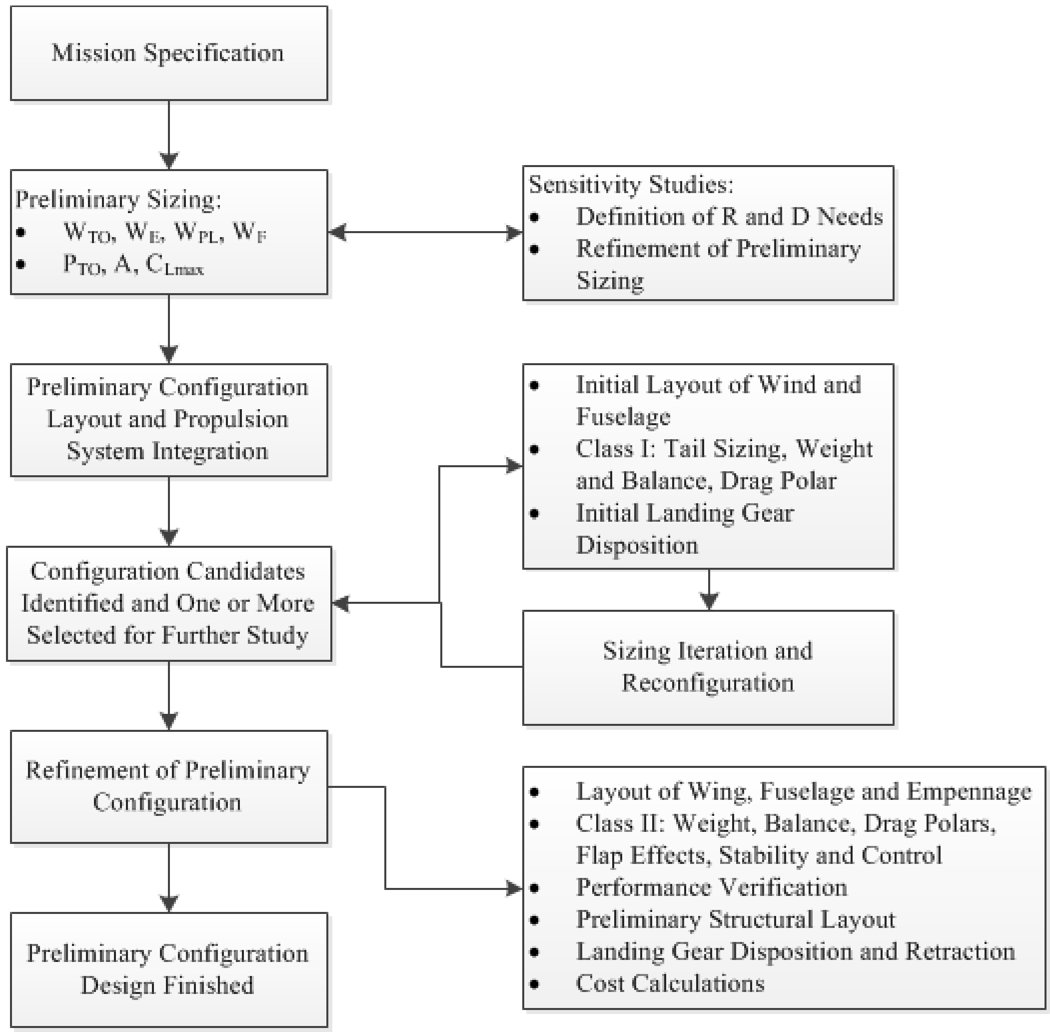


**Figure 1.5: Preliminary Design Sequence**

## 1.5 RENOSAUR DESIGN PHILOSOPHY

The Renosaur is designed to meet the Request for Proposal (RFP) given by the AIAA. In addition to meeting the requirements, the Renosaur is designed with the design philosophy explained in this section in mind. The primary goal is to win the Unlimited Class Race at Reno. This must be accomplished by combining a high top speed with an excellent maneuverability. To allow for a safety margin, and keeping in mind the current speed record in the Unlimited Class is 507 mph, the top speed of the Renosaur is set to be 600 mph. The Renosaur is primarily designed for the race mission. The ferry mission is considered where necessary, e.g. for the weight and balance presented in Chapter 6. The Renosaur will allow for extra fuel storage by using slipper tanks. The technical design approach is described in the design justification and technical approach presented in Section 2.The second major driver of the design is crashworthiness and public safety. The safety measures are explained in Section 1.6.

## 1.6 SAFETY MEASURES

The crashworthiness of the design is of even greater importance after the recent accident at the Reno Races in September 2011. The author recommends the organization of the Reno Races to move the public stands away from the race course to decrease the possibility of a crash into the public. Furthermore, the use of proximity sensors is recommended: if the aircraft is closer to the ground than a given distance, e.g. 200 ft, the aircraft will go into safe mode. In this safe mode, the aircraft will automatically pitch up and will not allow further descent. Another addition to this safety measure is automated landing. If the pilot is not able to control the aircraft, an emergency signal will be called out and GPS directed automated landing will be initiated. Since the aircraft has irreversible flight controls, as explained in Chapter 11, triple redundancy is used to assure safety. Furthermore, the flight controls are installed following FAR-25 requirements.

# 2 DESIGN JUSTIFICATION AND TECHNICAL APPROACH TO MEET MISSION REQUIREMENTS

This section presents the design justification and technical approach used to meet the mission requirements. The emphasis will lie on the approach used to fly far faster than current Unlimited Class racers.

## 2.1 WING AND POWER LOADING

Current Unlimited Class racers are mostly modified World War II fighters. A sizing chart of these aircraft is provided in Figure 2.1. As can be seen, most racers are designed for a wing loading in the range of 30 - 60 lbf/ft$^2$. These aircraft are designed approximately 70 years ago and not specifically for air racing. The design philosophy for these aircraft is focused on military use and not on completing the race track as fast as possible. Current technology allows for much higher top speeds and wing loadings.

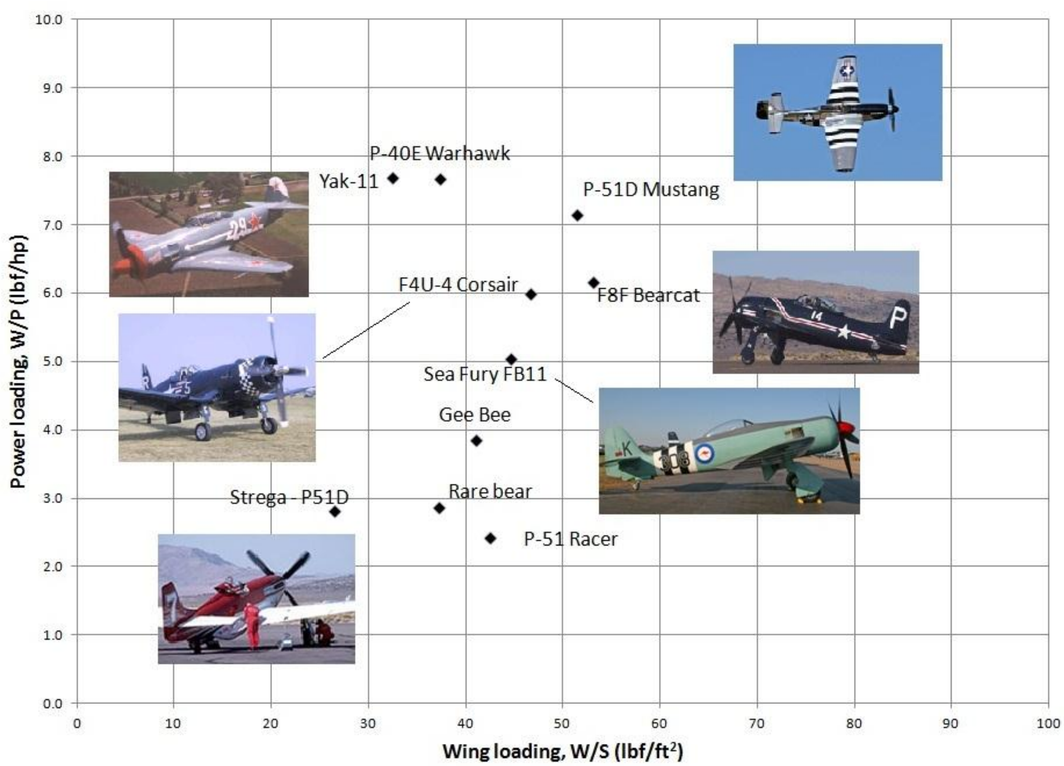


**Figure 2.1: Current Reno racers**

For the design of the Renosaur, it has been decided that the empty weight is set to the minimum allowable 4,500 lbf, to obtain a high wing and power loading. The author has decided to minimize the shaft power required. Considering an empty weight of 4,500 lbf, the Renosaur will scale down significantly with respect to the current racers. This will result in a much lower wetted area and thus a decrease in drag.

## 2.2 DESIGN SPACE SWEEP

To determine the overall configuration of the Renosaur the author has performed a sweep of the design space. The design of six different configurations and their wing planforms is documented.

The six configurations that have been considered are:

- Configuration a: Conventional
- Configuration b: Double fuselage with left cockpit
- Configuration c: Tandem wing
- Configuration d: Canard with double pusher
- Configuration e: Twin boom with tractor-pusher
- Configuration f: Twin boom with double tractor

Drawings of these configurations are produced in Shark FX and can be found in Figure 2.2 and 2.3.

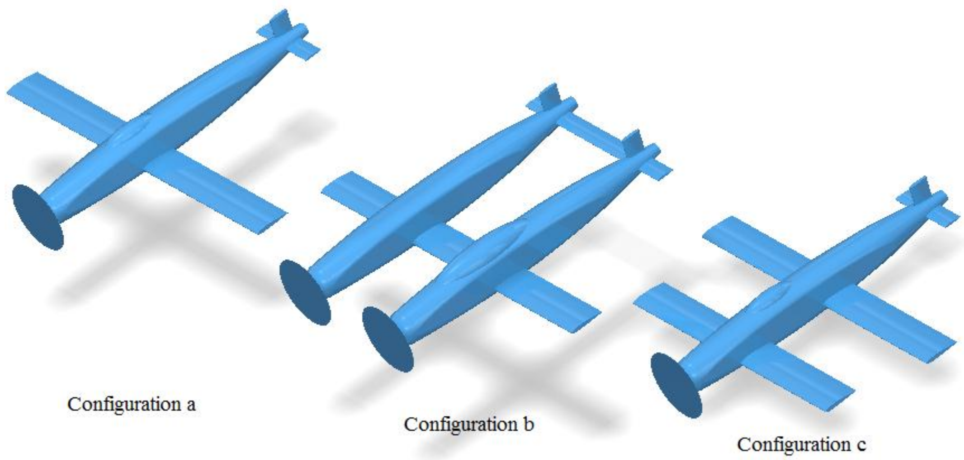


**Figure 2.2: Configuration a, b and c**

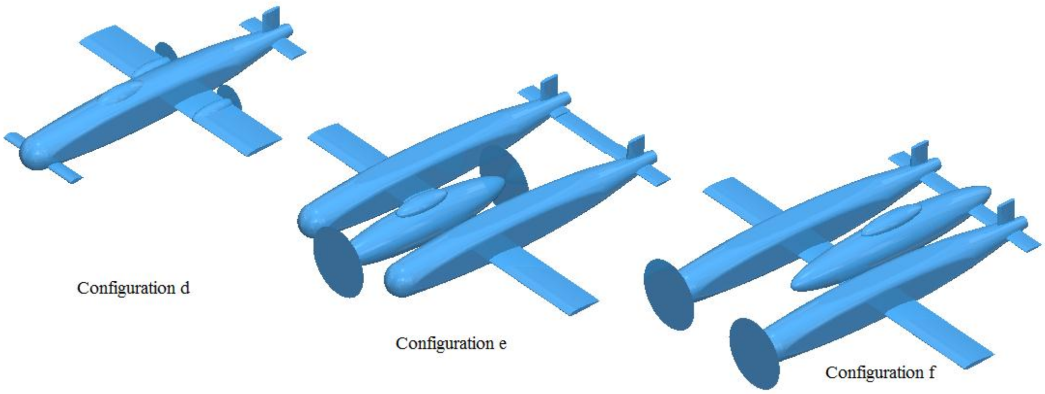


**Figure 2.3: Configuration d, e and f**

The wing planforms for the six configurations are varied for the range of the planform parameters presented in Table 2.1. The race lift coefficient and the aspect ratio are selected to be the primary design parameters; the other parameters are assumed to have a smaller influence on the design.

**Table 2.1: Wing planform sweep**

| **Wing planform parameters** | **Range** |
|---|---|
| Race lift coefficient, $C_{L_{max_{race}}}$ | 0.2 - 0.8 with increments of 0.2 |
| Aspect Ratio, $A$ | 2 – 8 with increments of 2 |
| Sweep angle, $\Lambda_{c/4}$ | - 45 – 45 degrees with increments of 15 degrees |
| Taper ratio, $\lambda$ | 0.3 – 0.5 with increments of 0.1 |

This sweep of the design space allows the designer to quickly change a design characteristic and investigate the influence this has on the other parameters. Varying the maximum race lift coefficient will change the wing loading and consequently the wing area, since the takeoff weight is fixed. The relation between the wing loading and the maximum lift coefficient is presented in Equation 2.1.

$$\frac{W}{S} = \frac{C_{L_{max}} \rho V^2}{2n} \qquad \text{(Equation 2.1)}$$

The wing loading versus power loading diagram for the range of race lift coefficients is presented in Figure 2.4. In this diagram it can be seen that the maneuver line reaches an asymptote around a power loading of 3 lbf/hp and a wing loading of 150 lbf/ft$^2$. Increasing the maximum lift coefficient, and therefore decreasing the wing area, does not result in a significant decrease in the total power near this asymptote. Therefore the design point is chosen at a wing loading where the corresponding power loading almost reaches the asymptote. This corresponds to a maximum lift coefficient of 0.5 in cruise.

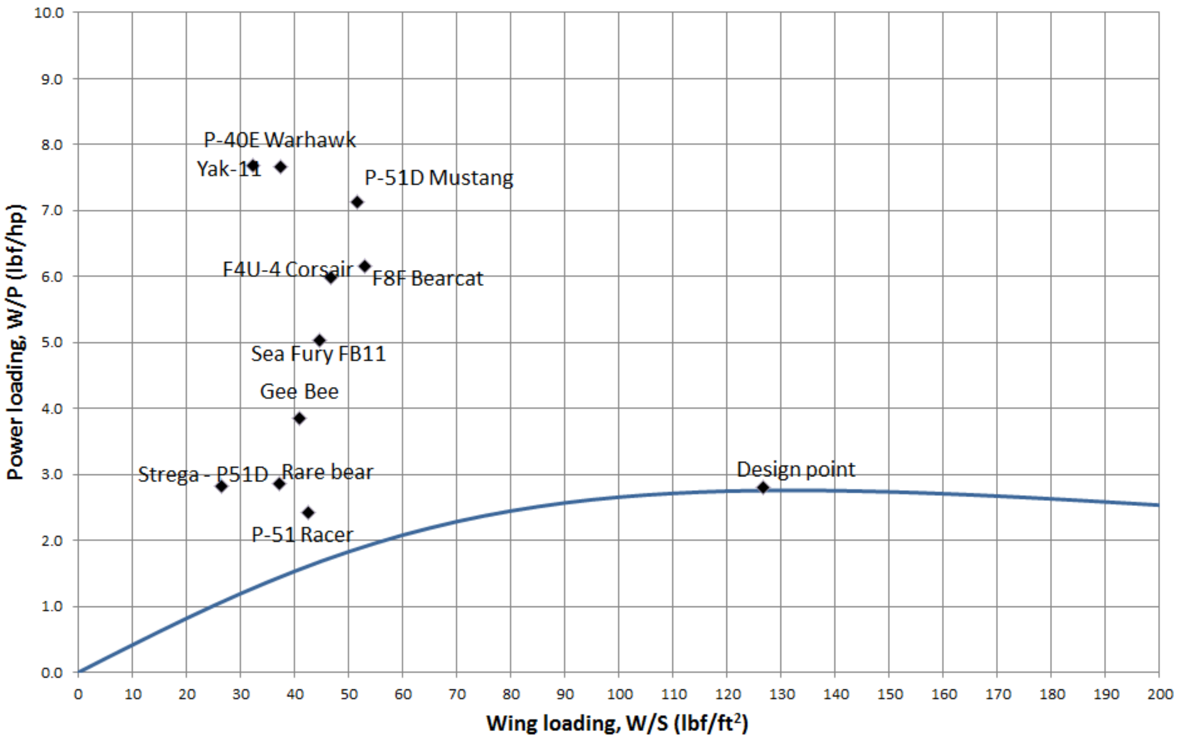


**Figure 2.4: Sizing diagram for the Renosaur**

The next step is to determine the aspect ratio. The aspect ratio will change the power loading if the wing loading is kept fixed, as can be seen in Equation 2.2.

$$\frac{W}{P} = \frac{2\left(\frac{W}{S}\right)550}{\rho V^3\left(C_{D_0} + \frac{\left(\frac{2nW}{\rho V^2 S}\right)^2}{\pi A e}\right)} \qquad \text{(Equation 2.2)}$$

The aspect ratio is selected to be 10, to decrease the total power needed. The unswept thickness to chord ratio is determined from Ref. 12. The Mach drag divergence number is related to the thickness ratio; this is shown in Figure 2.5 for a maximum lift coefficient of 0.5. As can be seen, advanced supercritical airfoils have a higher Mach drag divergence number and will therefore be used.

The Mach drag divergence number is selected to be 0.8. It is assumed that the Mach drag divergence dumber is slightly higher than the flight Mach number, to maintain low drag without decreasing the thickness ratio too much. This results in an unswept thickness to chord ratio of 12.7 percent. The swept thickness ratio relates to the unswept thickness ratio by Equation 2.3.

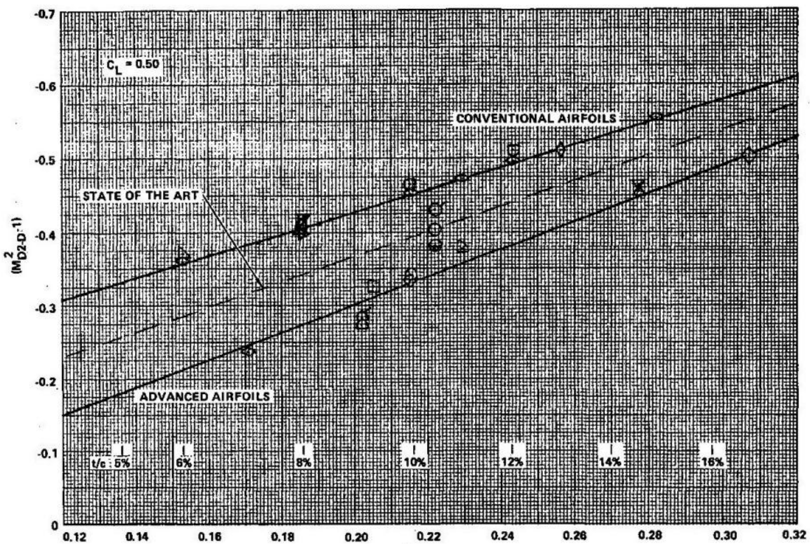

**Figure 2.5: Mach drag divergence number vs. Thickness ratio (Ref. 12)**

$$(t/c)_{swept} = (t/c)_{unswept} \cos(\Lambda_{c/4})$$ (Equation 2.3)

As Equation 2.3 shows, increasing the (forward or aft) sweep angle, will increase the thickness ratio. This increases the fuel volume that can be stored in the wing. The aft sweep angle is selected to be 20 degrees. Finally, an initial value of 0.5 for the taper ratio is selected. This is a common value for single engine propeller driven aircraft (Table 6.2, Ref. 5). The design parameters are summarized in Table 2.2.

**Table 2.2: Design parameters**

| | |
|---|---|
| Maximum lift coefficient, $C_{L_{max_{race}}}$ | 0.5 |
| Wing loading, W/S | 126.7 lbf/ft$^2$ |
| Power loading, W/P | 2.99 lbf/hp |
| Wing area, S | 40.8 ft$^2$ |
| Total power, P | 1732 hp |
| Aspect ratio, A | 10 |
| Mach drag divergence number, $M_{DD}$ | 0.8 |
| Sweep angle, $\Lambda_{c/4}$ | 20 degrees |
| Taper ratio, $\lambda$ | 0.5 |
| Thickness ratio, t/c | 0.127 |

# 3 CLASS I & II SIZING METHODS AND SENSITIVITIES

This Section documents the Class I and Class II sizing methods and sensitivities for the Renosaur. A description of similar airplanes is included, as well as the mission weights, sizing plot and weight sensitivities.

## 3.1 DESCRIPTION OF SIMILAR AIRPLANES

A description of eight similar airplanes is included. Since specifications of actual Reno racers were not always available, some stock versions of the racers are presented.

**Table 3.1: North American P-51D Mustang Specifications (Ref. 13)**

| | |
|---|---|
| Takeoff Weight | 12,100 lbf |
| Empty Weight | 7,635 lbf |
| Length | 32.3 ft |
| Height | 13.4 ft |
| Wing Span | 37 ft |
| Wing Area | 235 $ft^2$ |
| Fuel Capacity | n/a |
| Range | 1,650 mi |
| Cruise Speed | 362 mph |
| Maximum Speed | 437 mph |
| Stall Speed | 100 mph |
| Climb Rate | 3,200 ft/min |
| Service Ceiling | 41,900 ft |
| Engine | Packard V-1650-7 |
| Power | 1,695 hp |

**Table 3.2: Pond Racer PR-01 Specifications (Ref. 14)**


| | |
|---|---|
| Takeoff Weight | 4,150 lbf |
| Empty Weight | 3,500 lbf |
| Length | 20.0 ft |
| Height | 5.5 ft |
| Wing Span | 25.4 ft |
| Wing Area | n/a |
| Fuel Capacity | 84 gallons |
| Range | n/a |
| Cruise Speed | n/a |
| Maximum Speed | 530 mph |
| Stall Speed | n/a |
| Climb Rate | n/a |
| Service Ceiling | n/a |
| Engine | 2 VG-30 |
| Power | 2 x 1,000 hp |

**Table 3.3: Grumman F8F Bearcat Specifications (Ref. 13)**


| | |
|---|---|
| Takeoff Weight | 12,947 lbf |
| Empty Weight | 7,070 lbf |
| Length | 28.2 ft |
| Height | 13.8 ft |
| Wing Span | 35.8 ft |
| Wing Area | 244 $ft^2$ |
| Fuel Capacity | n/a |
| Range | 1,105 mi |
| Cruise Speed | 163 mph |
| Maximum Speed | 421 mph |
| Stall Speed | n/a |
| Climb Rate | 4,570 ft/min |
| Service Ceiling | 38,700 ft |
| Engine | 1 P&W R-2800 |
| Power | 2,100 hp |

**Table 3.4: Yakovlev Yak-11 (Ref. 15)**


| | |
|---|---|
| Takeoff Weight | 5,379 lbf |
| Empty Weight | 4,189 lbf |
| Length | 26.9 ft |
| Height | 10.8 ft |
| Wing Span | 30.8 ft |
| Wing Area | 166 $ft^2$ |
| Fuel Capacity | 795 mi |
| Range | 230 mph |
| Cruise Speed | 289 mph |
| Maximum Speed | n/a |
| Stall Speed | n/a |
| Climb Rate | 1,600 ft/min |
| Service Ceiling | 23,925 ft |
| Engine | 1 Shvetsox Ash-21 |
| Power | 700 hp |

**Table 3.5: Vought F4U-4 Corsair Specifications (Ref. 13)**


| | |
|---|---|
| Takeoff Weight | 14,670 lbf |
| Empty Weight | 9,205 lbf |
| Length | 33.5 ft |
| Height | 14.8 ft |
| Wing Span | 41.0 ft |
| Wing Area | 314 $ft^2$ |
| Fuel Capacity | n/a |
| Range | 1,005 mi |
| Cruise Speed | 215 mph |
| Maximum Speed | 446 mph |
| Stall Speed | n/a |
| Climb Rate | 3,870 ft/min |
| Service Ceiling | 41,500 ft |
| Engine | 1 P&W R-2800 |
| Power | 2,450 hp |

**Table 3.6: Hawker Sea Fury FB11 Specifications (Ref. 16)**

| | | |
|---|---|---|
|  | Takeoff Weight | 12,500 lbf |
| | Empty Weight | 9,240 lbf |
| | Length | 34.7 ft |
| | Height | 16.1 ft |
| | Wing Span | 38.4 ft |
| | Wing Area | 280 $ft^2$ |
| | Fuel Capacity | n/a |
| | Range | 700 mi |
| | Cruise Speed | 390 mph |
| | Maximum Speed | 460 mph |
| | Stall Speed | n/a |
| | Climb Rate | 2,780 ft/min |
| | Service Ceiling | 35,800 ft |
| | Engine | 1 Centaurus XVIIC |
| | Power | 2,480 hp |

**Table 3.7: Strega - P-51D Mustang Racer Specifications (Ref. 17)**

| | | |
|---|---|---|
|  | Takeoff Weight | 10,000 lbf |
| | Empty Weight | 7,800 lbf |
| | Length | 32.25 ft |
| | Height | 8.75 ft |
| | Wing Span | 32.4 ft |
| | Wing Area | 200 $ft^2$ |
| | Fuel Capacity | n/a |
| | Range | n/a |
| | Cruise Speed | 388 mph |
| | Maximum Speed | 460 mph |
| | Stall Speed | n/a |
| | Climb Rate | 3,200 ft/min |
| | Service Ceiling | 41,900 ft |
| | Engine | Rolls Royce V-1650 |
| | Power | 3600 hp |

**Table 3.8: Goodyear F2G "Super" Corsair (Ref. 18)**

| | | |
|---|---|---|
|  | Takeoff Weight | 15,422 lbf |
| | Empty Weight | 10,249 lbf |
| | Length | 27.9 ft |
| | Height | 7.84 ft |
| | Wing Span | 30.18 ft |
| | Wing Area | 159.8 $ft^2$ |
| | Fuel Capacity | n/a |
| | Range | 405 mi |
| | Cruise Speed | n/a |
| | Maximum Speed | 407 mph |
| | Stall Speed | n/a |
| | Climb Rate | 3,645 ft/min |
| | Service Ceiling | 35,000 ft |
| | Engine | Klimov VK-105PF-2 |
| | Power | 1,300 hp |

## 3.2 MISSION WEIGHTS

To be able to determine the takeoff weight of the Renosaur, the regression constants A and B need to be determined. This is done using a database with the takeoff weight and empty weight of similar aircraft, given in Table 3.9. The relation between these weights is given in Figure 3.1. With this data a linear regression plot is produced, which is shown in Figure 3.2.

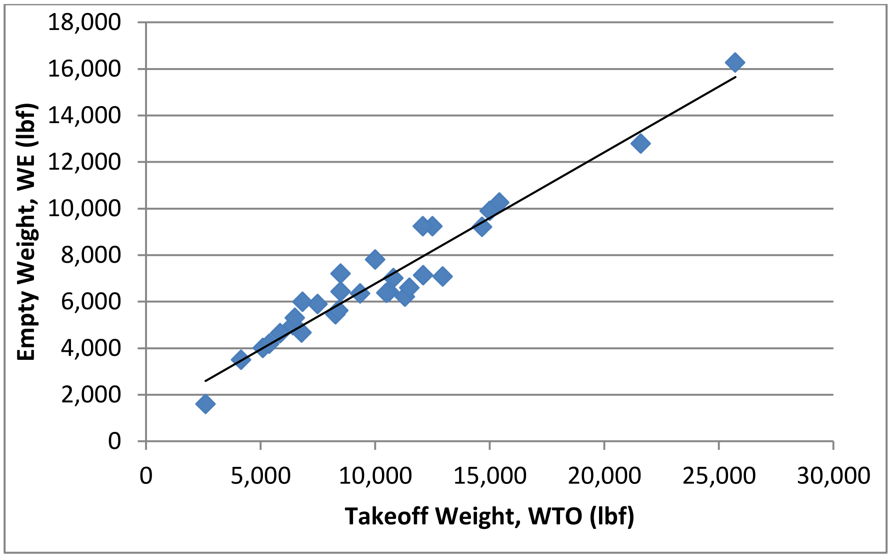


**Figure 3.1: Takeoff weight vs. Empty weight for similar airplanes**

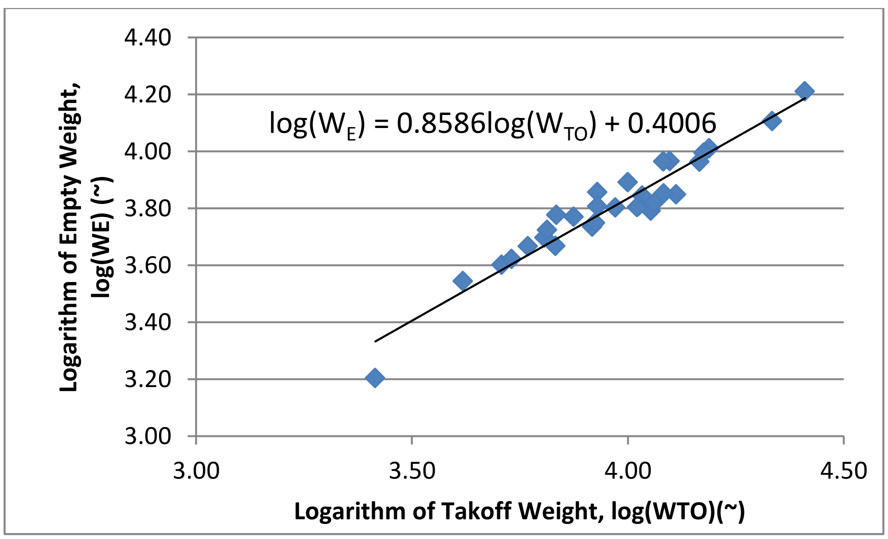


**Figure 3.2: Linear regression plot**

**Table 3.9: Aircraft database**

| | |
|---|---|
| 1 | Dago Red - P51D |
| 2 | F2G-1 Corsair |
| 3 | F4U-4 Corsair |
| 4 | F7F-3 Tigercat |
| 5 | F8F-1 Bearcat |
| 6 | FM-2 Wildcat |
| 7 | FW-190A |
| 8 | Hawker Sea Fury |
| 9 | MB 5 |
| 10 | Me 109 |
| 11 | Nemesis NXT |
| 12 | P-38L Lightning |
| 13 | P-39M Airacobra |
| 14 | P-40E |
| 15 | P-40N |
| 16 | P-47D Thunderbolt |
| 17 | P-51A Mustang |
| 18 | P-51D Mustang |
| 19 | P-51H Mustang |
| 20 | P-63 Kingcobra |
| 21 | P-64 |
| 22 | Pond Racer PR-01 |
| 23 | Spitfire Mk VA |
| 24 | Steadfast - Yak 3U |
| 25 | Strega - P51D |
| 26 | T-28B Trojan |
| 27 | Tsunami |
| 28 | Yak-11 |
| 29 | Yak-3 |
| 30 | Yak-9U |

The relation between the logarithmic value empty weight and the takeoff weight is given in Equation 3.1. The regression constants A and B are calculated in the Advanced Aircraft Analysis (AAA) program. The values of the regression constants are documented in Table 3.10.

$$W_E = 10^{\frac{\log(W_{TO})-A}{B}}$$ (Eq. 3.1) (Eq. 2.16, Ref. 4)

**Table 3.10: Regression constants**

| | A | B |
|---|---|---|
| AAA | -0.12 | 1.07 |

Using Equation 3.1 and fixing the empty weight at 4500 pounds, the takeoff weight is determined to be 6345 lbf. However, an alternative method is used to determine the mission weights. In this method, the aircraft database and the regression line are not used. Since almost all aircraft in this database are designed to carry a payload, the data is less useful for the design of the Renosaur. The alternative method is performed to start with a clean sheet and compare the values found from this method to the regression method. In the design process of the Renosaur, the decision has been made to minimize the empty weight of the aircraft. The minimum empty weight specified by the AIAA is 4,500 lbf. This value has been taken as an estimate for the empty weight. The following mission weights are already known:

- Empty weight: 4,500 lbf (assumed)
- Payload weight: 0 lbf (no payload)
- Crew weight: 200 lbf (one pilot)

The next step is to determine what the fuel weight would be for these mission weights and different combinations of propulsive efficiency, specific fuel consumption and lift-to-drag ratio during the race. The procedure is only performed for the cruise phase, since that phase will define if the Renosaur will win the race. In Table 3.11 the range for the parameters that have been considered is presented.

**Table 3.11: Tested range for parameters of Breguet Range equation.**

| **Parameter** | **Range** |
|---|---|
| Propulsive efficiency, $\eta_p$ | 0.5 – 0.9 with increments of 0.1 |
| Specific fuel consumption, $c_p$ | 0.5 – 1.0 with increments of 0.1 |
| Lift-to-Drag ratio, L/D | 2 – 10 with increments of 2. |

Using the fuel fractions method outlined in Ref. 4, the total mission weights and cruise performance parameters are presented in Table 3.12. This process is performed in the AAA program. The value for the takeoff weight includes a 100 lbf increase in structural weight to account for crashworthiness.

**Table 3.12: Design parameters**

| | |
|---|---|
| Propulsive efficiency, $\eta_p$ | 0.7 |
| Specific fuel consumption, $c_p$ | 0.5 lbf/(hp-hr) |
| Lift-to-Drag ratio, L/D | 8 |
| Empty weight, $W_E$ | 4,500 lbf |
| Takeoff weight, $W_{TO}$ | 5,175 lbf |
| Fuel weight, $W_F$ | 98 lbf |
| Crew weight, Wcrew | 200 lbf |

## 3.3 WEIGHT SENSITIVITIES

The method used to determine the takeoff weight sensitivities deviates from the method outlined in Ref. 2. The approach used to determine the mission weights is expanded to include the weight sensitivities. The parameters selected for the propulsive efficiency, specific fuel consumption and lift-to-drag ratio for the cruise phase are varied in AAA. The differences these changes cause to the takeoff weight are documented. Once again, this has only been done for the cruise phase, since this phase will define the performance of the racer. The assumption is made that the difference in takeoff weight with respect to a certain parameter $x$, $\frac{\Delta W_{TO}}{\Delta x}$, is the same as the partial differential $\frac{\partial W_{TO}}{\partial x}$. To get a feeling for the relative importance of the sensitivities, they are normalized to obtain sensitivities with same order of magnitude. The sensitivities are presented in Table 3.13

**Table 3.13: Takeoff weight sensitivities**

| | Design values | Design takeoff weight, $W_{TO}$ | Increase in values | Changed takeoff weight, $W_{TO}$ | $\frac{\delta W_{TO}}{\delta x}$ | $\left(\frac{\Delta W_{TO}}{\Delta x}\right)_{normalized}$ |
|---|---|---|---|---|---|---|
| $L/D$ | 8 | 5075 lbf | 0.5 | 5070 lbf | -10 lbf | -5 lbf |
| $c_p$ | 0.5 lbf/(hp-hr) | 5075 lbf | 0.1 lbf/(hp-hr) | 5092 lbf | 170 lbf/(lbf/hp-hr) | 17 lbf/(lbf/hp-hr) |
| $\eta_p$ | 0.7 | 5075 lbf | 0.1 | 5064 lbf | -110 lbf | -11 lbf |
| $R$ | 58.2 nmi | 5075 lbf | 10 nmi | 5083 lbf | 0.8 lbf/nmi | 8 lbf/nmi |

The takeoff weight is most sensitive to a change in specific fuel consumption and propeller efficiency. The takeoff weight is least sensitive to a change in the lift-to-drag ratio. This means that a change in the specific fuel consumption or the propeller efficiency needs to be avoided, since this will cause a significant change in the takeoff weight.

The weight sensitivities for the climb and loiter phases are determined in AAA. However, this method is based on the regression constant B, which is not used to determine the mission weights. Therefore, these values can be used as a sanity check, but have limited validity. The takeoff weight sensitivities determined in AAA are given in Fig. 3.3.

**Input Parameters**

| | | | | | | | | |
|---|---|---|---|---|---|---|---|---|
| $B$ | 1.0725 | | $W_{PL}$ | 0.0 | lb | $M_{tfo}$ | 0.500 | % |
| $M_{ff}$ | 0.9296 | | $W_{crew}$ | 200.0 | lb | $M_{F_{res}}$ | 0.000 | % |
| $W_{TO}$ | 5175.0 | lb | | | | | | |
| $W_E$ | 4500.0 | lb | | | | | | |

**Output Parameters**

| | | | | | |
|---|---|---|---|---|---|
| $\partial W_{TO}/\partial W_{PL}$ | 10.15 | $\partial W_{TO}/\partial W_{crew}$ | 10.15 | $\partial W_{TO}/\partial W_E$ | 1.23 |

**Mission Sensitivity Table: Output**

| | Mission Profile | $\partial W_{TO}/\partial W_{FL_{exp}}$ | $\partial W_{TO}/\partial W_{F_{refuel}}$ | $\partial W_{TO}/\partial c_p$ hp-hr | $\partial W_{TO}/\partial R$ lb/nm | $\partial W_{TO}/\partial L/D$ lb | $\partial W_{TO}/\partial E$ lb/hr | $\partial W_{TO}/\partial \eta_p$ lb |
|---|---|---|---|---|---|---|---|---|
| 1 | Warmup | | | | | | | |
| 2 | Taxi | | | | | | | |
| 3 | Take-off | | | | | | | |
| 4 | Climb | | | 4.7 | | -0.3 | 3371.1 | -3.5 |
| 5 | Loiter | | | 936.4 | | -56.2 | 3371.1 | -702.3 |
| 6 | Cruise | | | 1717.3 | 12.6 | -101.0 | | -1226.7 |
| 7 | Loiter | | | 624.3 | | -37.5 | 2247.4 | -468.2 |
| 8 | Descent | | | | | | | |
| 9 | Land/Taxi | | | | | | | |

**Figure 3.3: AAA Weight Sensitivities**

## 3.4 SIZING PLOT

The sizing plot of the Renosaur is presented in Figure 3.4.

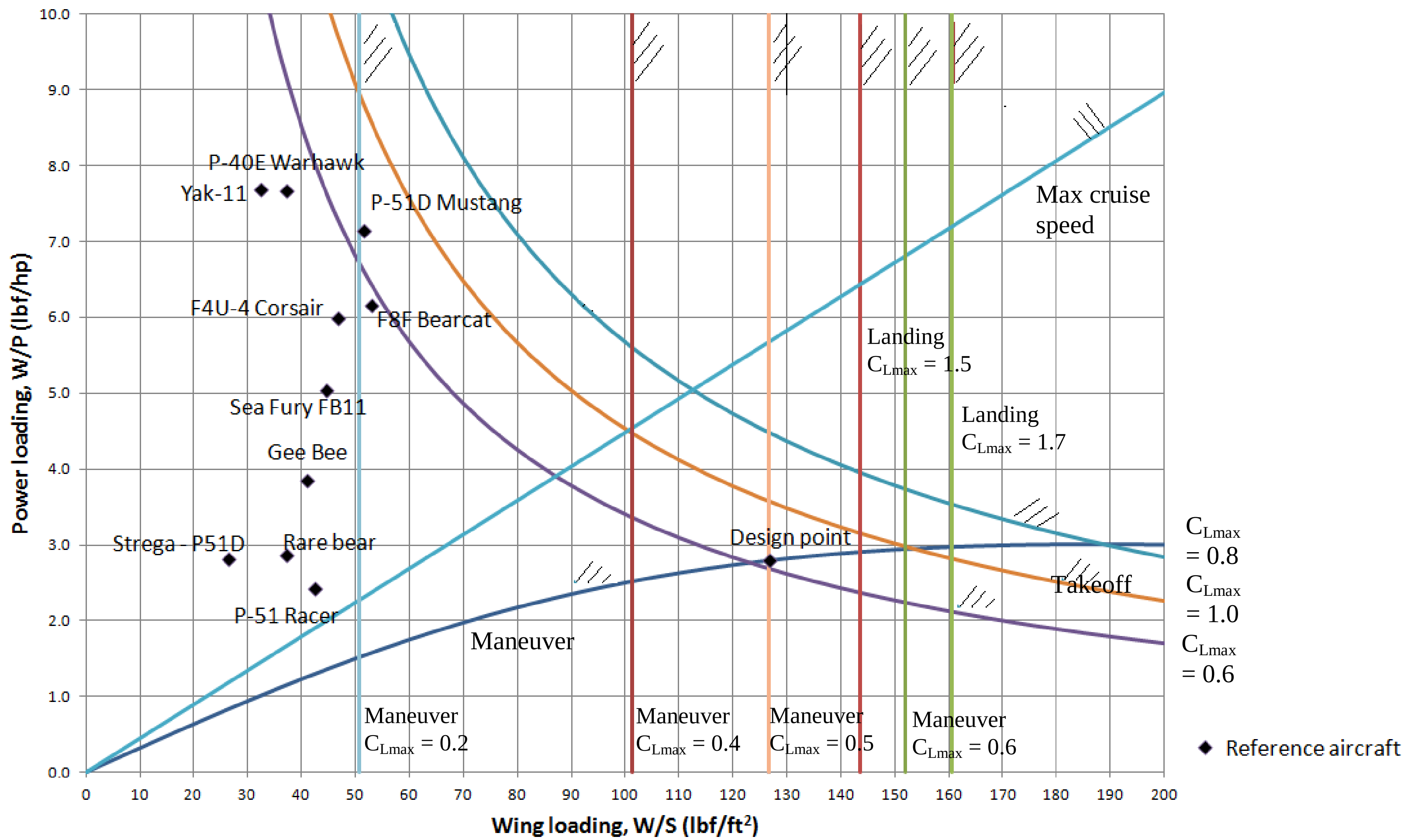


**Figure 3.4: Wing Sizing Diagram for the Renosaur**

# 4 THREE-VIEW OF THE GENERAL ARRANGEMENT AND SALIENT CHARACTERISTICS

This Section presents the three-view of the Renosaur, as well as the aircraft geometry and the salient characteristics. The isometric view of the Renosaur is given in Figure 4.1; an in-flight view is presented in Figure 4.2.

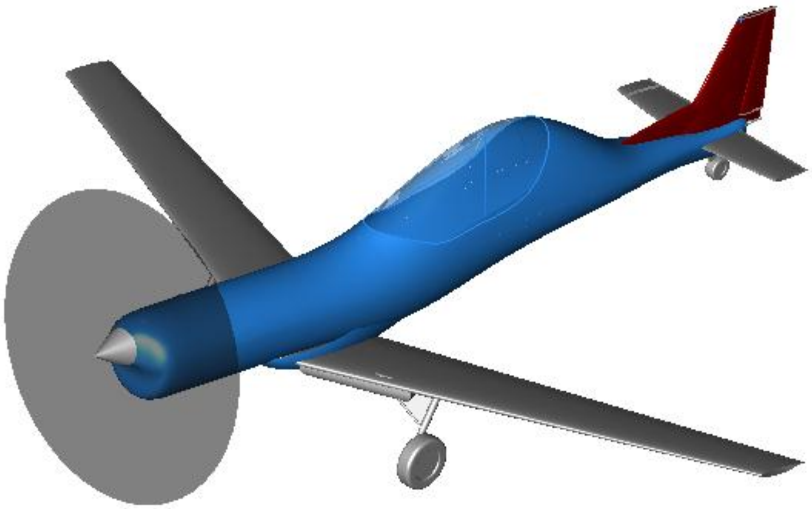

**Figure 4.1: Isometric View of the Renosaur**

**Figure 4.2: Isometric View of the Renosaur in flight**

The three-view of the Renosaur is presented in Figure 4.3.

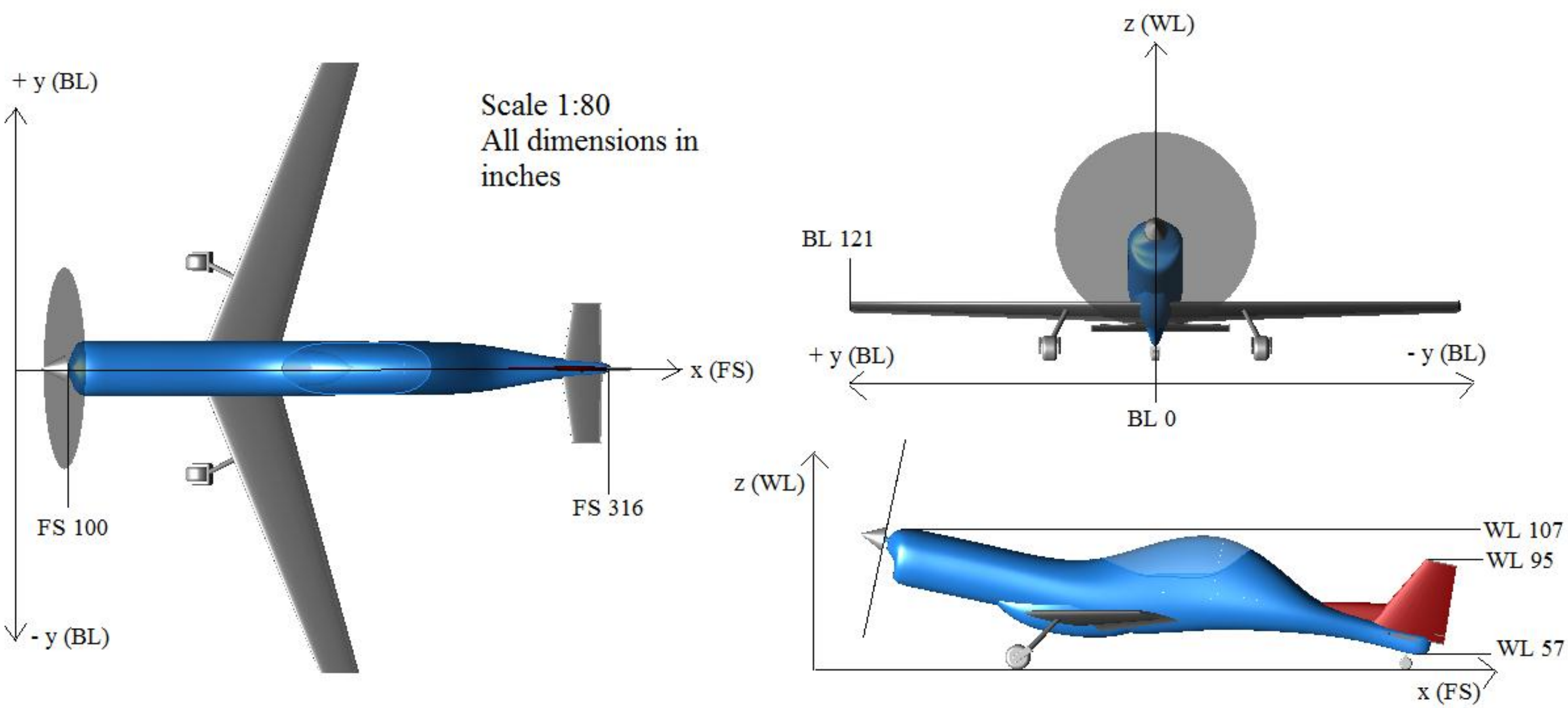


**Figure 4.3: Three-View of the Renosaur**

**Table 4.1: Renosaur Geometric Characteristics**

| | **Wing** | **Horizontal Tail** | **Vertical Tail** |
|---|---|---|---|
| Area | 40.8 $ft^2$ | 4.2 $ft^2$ | 3.4 $ft^2$ |
| Span | 20.2 ft | 4.6 ft | 2.6 ft |
| Mean Geometric Chord | 2.1 ft | 0.9 ft | 1.4 ft |
| MGC Leading Edge FS | 14.75 ft | 24.7 ft | 24.4 ft |
| Aspect Ratio | 10 | 5 | 2 |
| Sweep Angle (c/4) | 20 deg | 5 deg | 30 deg |
| Taper Ratio | 0.5 | 0.7 | 0.4 |
| Thickness Ratio | 0.147 | 0.12 | 0.12 |
| Airfoil | SC(2)-0714 | SC(2)-0712 | SC(2)-0712 |
| Dihedral Angle | 5 deg | 0 deg | 90 deg |
| Incidence Angle | 2 deg | 0 deg | 0 deg |
| Elevator Chord Ratio | | 0.35 | |
| Rudder Chord Ratio | | | 0.4 |
| | **Fuselage** | | |
| Length | 18.0 ft | | |
| Maximum Height | 3.1 ft | | |
| Maximum Width | 2.1 ft | | |

The Renosaur is a highly maneuverable, single-seat aircraft with a top speed of 600 miles per hour. It is designed to compete in the Unlimited Class in the Reno Air Races. The Renosaur uses two BMW P84 engines producing 900 shaft horsepower each. It has a range of 500 nautical miles in ferry condition, using slipper tanks. The Renosaur is a conventional configured aircraft with a tractor engine, cantilever low wing and fuselage mounted empennage. The landing gear is a retractable taildragger configuration.

# 5 INBOARD PROFILE AND CLASS II DESIGN

This Section presents the inboard profile as well as the Class II design of the Renosaur.

## 5.1 OVERALL CONFIGURATION

The overall configuration of the Renosaur is conventional. The reasons for selecting this configuration are as follows:

- Low wetted area contribution of the fuselage
- Keep the thrust on the aircraft on the centerline
- Sufficient data is available on conventional configurations

## 5.2 FUSELAGE CONFIGURATION

The fuselage configuration is selected to be conventional. The fuselage dimensions are given in Table 5.1 and determined following the method outlined in Ref. 5.

**Table 5.1: Fuselage dimensions**

| | |
|---|---|
| $l_f$ | 216 in |
| $l_{fc}$ | 100 in |
| $d_f$ | 31 in |
| $\theta_{fc}$ | 15 deg |
| $l_f/d_f$ | 6.97 |
| $l_{fc}/d_f$ | 3.22 |

## 5.3 ENGINE CONFIGURATION

The engines currently used in the Unlimited Class are mostly modified engines designed around the 1930's. To obtain better specific fuel consumption and a higher efficiency, the author has looked into Formula One car engines and has selected two BMW P84/5 engines, in an in-line configuartion. The engine can be seen in Figure 5.1 (Ref 19).


**Figure 5.1: BMW P84/5 engine (Ref. 19)**

These engines are connected in an in-line configuration in the forward fuselage. This engine is selected because it has significantly smaller dimensions and weight, as can be seen in the BMW P84/5 specifications presented in Table 5.2. Two BMW P84/5 engines produce 1850 bhp, which is more than the 1723 bhp needed. As presented in Table 5.2, the engine speed is 19,000 rpm. Since most piston aircraft engines run at approximately 3,000 rpm a gear reduction mechanism is necessary. In this stage of the design, the gear reduction of the Garrett TPE331 is selected for this purpose. Half of the length and weight of the TPE331 is added to the two BMW P84/5 engines to obtain the overall dimensions and weight of the propulsion installation. The specifications of the TPE331 and the overall dimensions of the propulsion system can be found in Table 5.3.

**Table 5.2: BMW P84/5 Specs (Ref. 19)**

| | |
|---|---|
| Engine type | BMW P84/5 V10 |
| Cylinders | 10 |
| Displacement | 2998 cc |
| Weight | 203 lbf |
| Height | 12.6 in |
| Width | 21.06 in |
| Length | 22.78 in |
| Brake horsepower | 925 bhp |
| Engine speed | 19,000 rpm |

**Table 5.3: Propulsion System Specs**

| | |
|---|---|
| **Garrett TPE331 (Ref. 20)** | |
| Weight | 336 lbf |
| Length | 46 in |
| Height | 21 in |
| Width | 21 in |
| **Overall propulsion system** | |
| Weight | 574 lbf |
| Length | 68.6 in |
| Height | 21 in |
| Width | 21 in |

## 5.4 WING CONFIGURATION

As stated in Section 2, a supercritical airfoil will be used for the Renosaur. The NACA SC(2)-0714 airfoil is selected. The wing planform parameters are given in Table 5.4.

The forward and aft spar will be located at 0.1c and 0.7c, respectively. The high maximum lift coefficient of the airfoil eliminates the use of flaps or slats. An estimated wing fuel volume of 4.5 $ft^3$ is determined. The wing planform including aileron is presented in Figure 4.2.

**Table 5.4: Planform parameters**

| | |
|---|---|
| Wing area, S | 40.8 $ft^2$ |
| Aspect Ratio, A | 10 |
| Sweep angle, $\Lambda_{c/4}$ | -20 deg |
| Wing span, b | 20.2 ft |
| Root chord, $c_r$ | 2.69 ft |
| Tip chord, $c_t$ | 1.35 ft |
| Taper ratio, $\lambda$ | 0.5 |
| Incidence angle, i | 2 deg |
| Dihedral angle, $\Gamma$ | 5 deg |
| Thickness ratio, t/c | 0.127 |

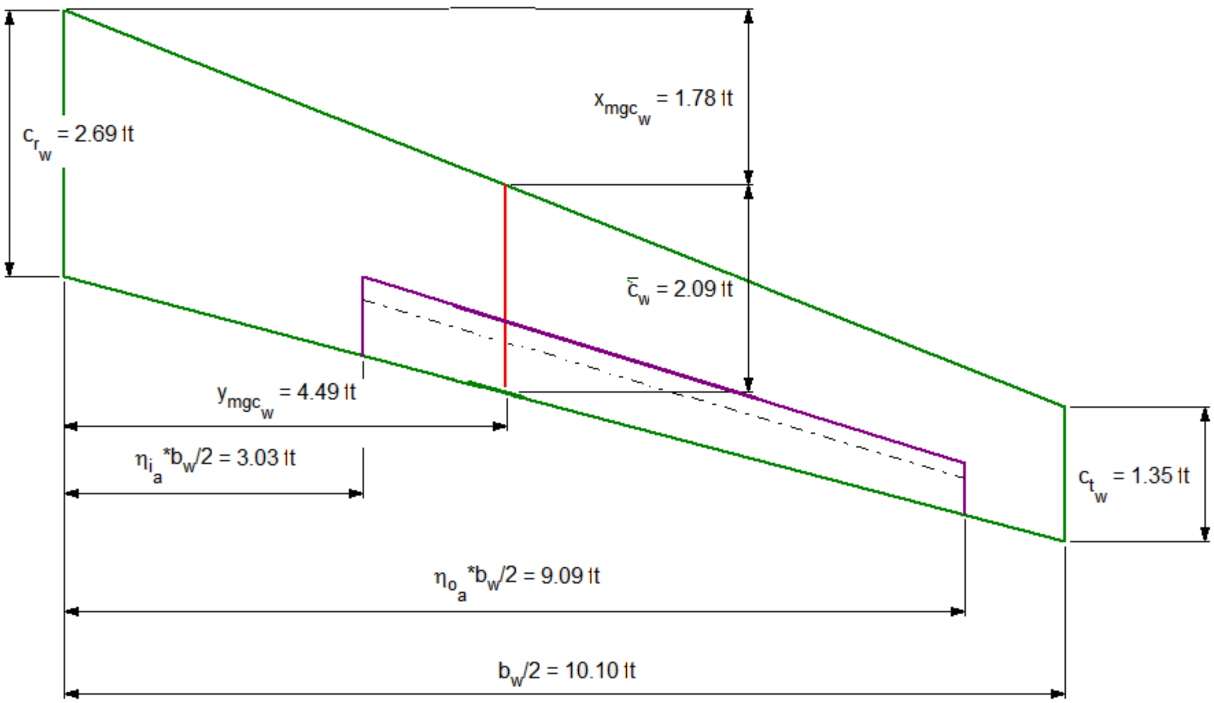


**Figure 4.2: Wing Planform Geometry**

## 5.5 EMPENNAGE CONFIGURATION

The empennage is selected to be a conventional configuration. It was first sized using the volume coefficient method (Ref. 4), and later resized during the Stability and Control analysis. Horizontal and vertical tail parameters are shown in Table 5.5. The elevator and rudder parameters are presented in Table 5.6. The final horizontal and vertical tail areas are:

- Horizontal tail: 4.2 $ft^2$
- Vertical tail: 3.4 $ft^2$

**Table 5.5: Empennage parameters**

| | Horizontal Tail | Vertical Tail |
|---|---|---|
| A | 5 | 1.4 |
| $\Lambda_{c/4}$ | 5 ° | 30 ° |
| λ | 0.7 | 0.4 |
| t/c | 15 % | 15 % |
| airfoil | NACA 0010 | NACA 0010 |
| Γ | 0 ° | 90 ° |
| i | 0° | 0 ° |

**Table 5.6: Elevator and rudder parameters**

| **Elevator** | | **Rudder** | |
|---|---|---|---|
| $S_e/S_h$ | 0.34 | $S_r/S_v$ | 0.34 |
| $S_e$ | 2.0 $ft^2$ | $S_r$ | 1.17 $ft^2$ |
| $c_e/c_h$ | 0.35 | $c_r/c_v$ | 0.4 |
| $c_e$ | 0.41 ft | $c_r$ | 0.53 ft |
| $\eta_{ie}$ | 10 % | $\eta_{ir}$ | 10 % |
| $\eta_{oe}$ | 100 % | $\eta_{or}$ | 100 % |

## 5.6 LANDING GEAR CONFIGURATION

The landing gear configuration for the Renosaur is a retractable taildragger configuration. The tires are sized for Type 2 Surfaces. The tires are selected from Tables 2.5 – 2.16, Ref. 7 and their parameters are given in Table 5.7.

**Table 5.7: Tire selection**

| | $D_0$ (in) | Width (in) | Type | Max. Loading (lbf) | Max. Speed (mph) | Weight (lbf) | Pressure (psi) |
|---|---|---|---|---|---|---|---|
| Main gear | 18 | 4.4 | VII | 4350 | 300 | 11.5 | 225 |
| Tail gear | 16 | 4.4 | VII | 1100 | 200 | 7.5 | 55 |

Type VIII tires are selected for the Renosaur because this type is especially suitable for aircraft with a high takeoff and landing speeds. The loads on the main and tail gear are determined with the method shown in Fig. 2.22, Ref. 7. The loads are determined to be:

- Main landing gear:
  - Maximum static load: 3044 lbf
- Tail landing gear:
  - Minimum static load: 381 lbf
  - Maximum static load: 461 lbf
  - Dynamic load: 750 lbf

**Table 5.8: Strut and Shock Absorber dimensions**

| Strut length | | Shock absorber length | |
|---|---|---|---|
| Main strut | 26 in | Main gear | 9.6 in |
| Tail strut | 10 in | Tail gear | 3.0 in |

In these loads a safety factor of 1.25 is included to allow for growth in the airplane weight. The gear struts were sized by following the Class II method presented in Chapter 2, Ref. 8. The lengths of the struts and shock absorbers are given in Table 5.8. The tip-over and ground clearance criteria for the Renosaur are satisfied. This can be seen in Figure 5.3, Figure 5.4 and Figure 5.5.

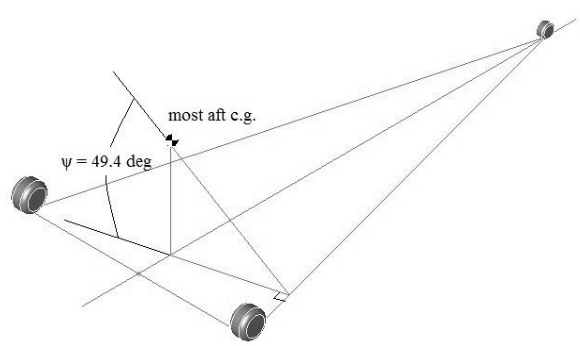


**Figure 5.3: Lateral Tip-Over Criterion**

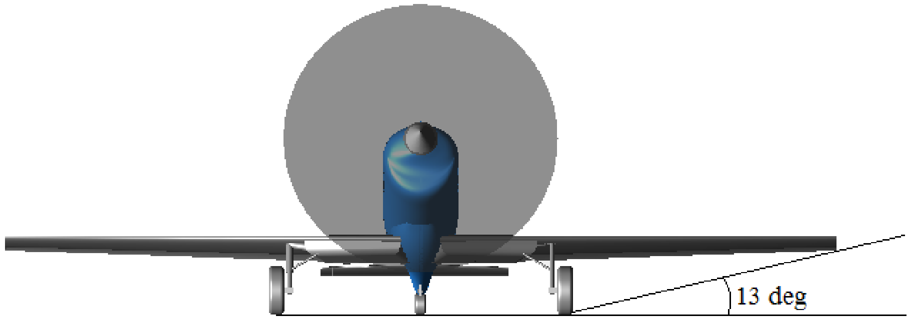


**Figure 5.4: Lateral Ground Clearance Criterion**

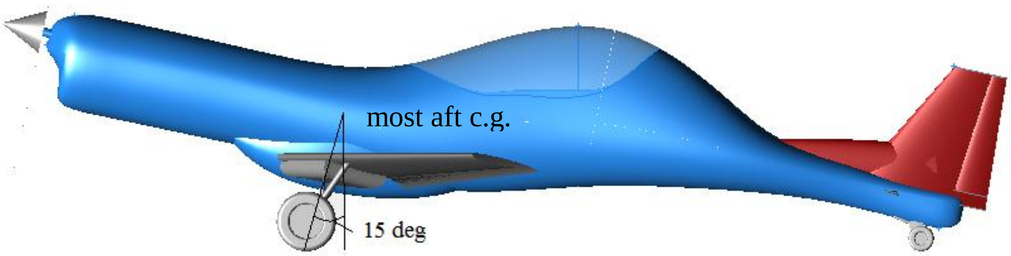


**Figure 5.5: Longitudinal Tip-Over Criterion**

An isometric view of the retracted landing gear in flight is given in Figure 5.6

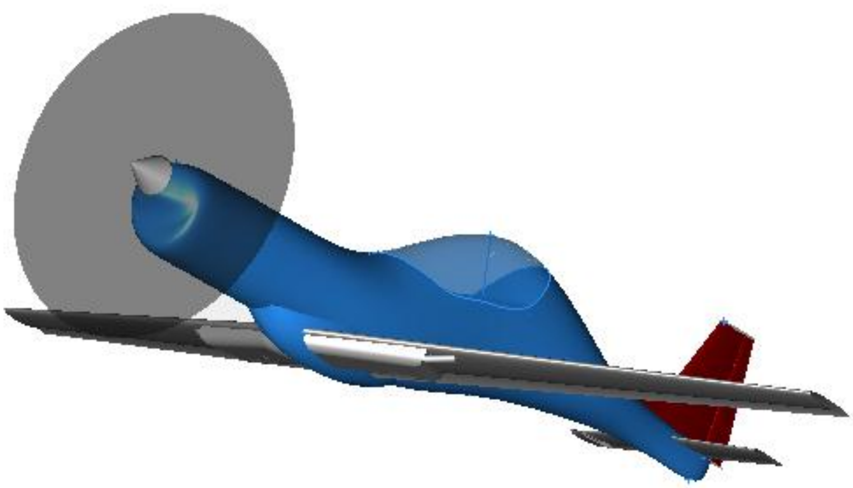

**Figure 5.6: Isometric view of the Retracted Landing Gear**

# 6 CLASS II WEIGHT AND BALANCE

This Section documents the Class II Weight and Balance for the Renosaur. The methods used for the Class II Weight and Balance can be found in Ref. 8.

## 6.1 CLASS II WEIGHT AND BALANCE CALCULATIONS

The Class II Weight calculations are performed in AAA. The component weights determined from AAA gave an empty weight that was too low for the Reno Air Races. The author has decided to use higher weights for the structural components in this design stage. Since the structure is reinforced with tungsten (see Section 10), the weight of the structural components will increase. If this weight margin is needed for other components in a later design stage, the structural weights will be recalculated. The Class II design weights can be summarized as presented in Table 6.1. The Class II moments of inertia are determined with the equations presented in Chapter 10, Ref. 8. The moments of inertia $I_{xy}$ and $I_{yz}$ are zero since the Renosaur is a symmetrical airplane. The moments of inertia of the Renosaur are presented in Table 6.2. The breakdown of the takeoff weight is also given in Figure 6.1.

**Table 6.1: Class II design weights**

| | |
|---|---|
| Empty weight | |
| Structural weight | 2206 lbf |
| Propulsion weight | 1542 lbf |
| Fixed equipment weight | 1103 lbf |
| Crew weight | 200 lbf |
| Payload weight | 0 lbf |
| Trapped fuel and oil | 26 lbf |
| Fuel weight | 97.5 lbf |

**Table 6.2: Moments of Inertia**

| | |
|---|---|
| Ixx | $5.93 \times 10^5$ lbf/in$^2$ |
| Iyy | $9.68 \times 10^7$ lbf/in$^2$ |
| Izz | $1.08 \times 10^7$ lbf/in$^2$ |
| Izx | $1.84 \times 10^6$ lbf/in$^2$ |

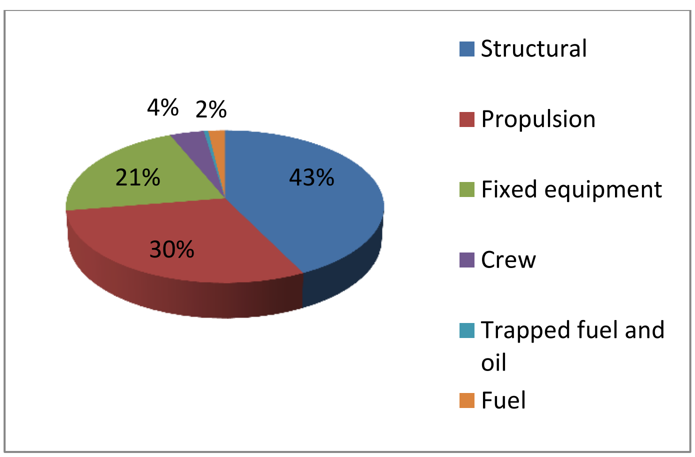


**Figure 6.1: Weight Breakdown**

The detailed Class II weight breakdown is presented in Table 6.3.

**Table 6.3: Renosaur Component Weights**

| **Aircraft Component** | **Weight (lbf)** |
|---|---|
| Wing group | 800 |
| Empennage group | 190 |
| Fuselage group | 800 |
| Nacelle group | 0 |
| Landing gear group | 416 |
| **Structure total** | **2206** |
| Propeller | 477 |
| Engine | 600 |
| Fuel system | 230 |
| Air Induction system | 64 |
| Propulsion System | 171 |
| **Power plant total** | **1542** |
| Flight Control system | 359 |
| Hydraulic system | 31 |
| Instruments, Avionics and Electronic Equipment | 127 |
| Air-conditioning, Pressurization, Anti-icing and De-icing System | 89 |
| Auxiliary Power | 41 |
| Electrical System | 252 |
| Oxygen Systems | 16 |
| Furnishings | 162 |
| Paint | 26 |
| **Fixed Equipment Total** | **1103** |
| Trapped Fuel and Oil | 26 |
| Fuel | 98 |
| Payload | 0 |
| Crew | 200 |
| **Takeoff weight** | **5175** |

## 6.2 CLASS II CG POSITIONS ON THE AIRFRAME, CG EXCURSION

The c.g. location for each component presented in Table 6.4 is estimated and indicated on the three-view presented in Figure 6.2. The numbering is also defined in Table 6.4.

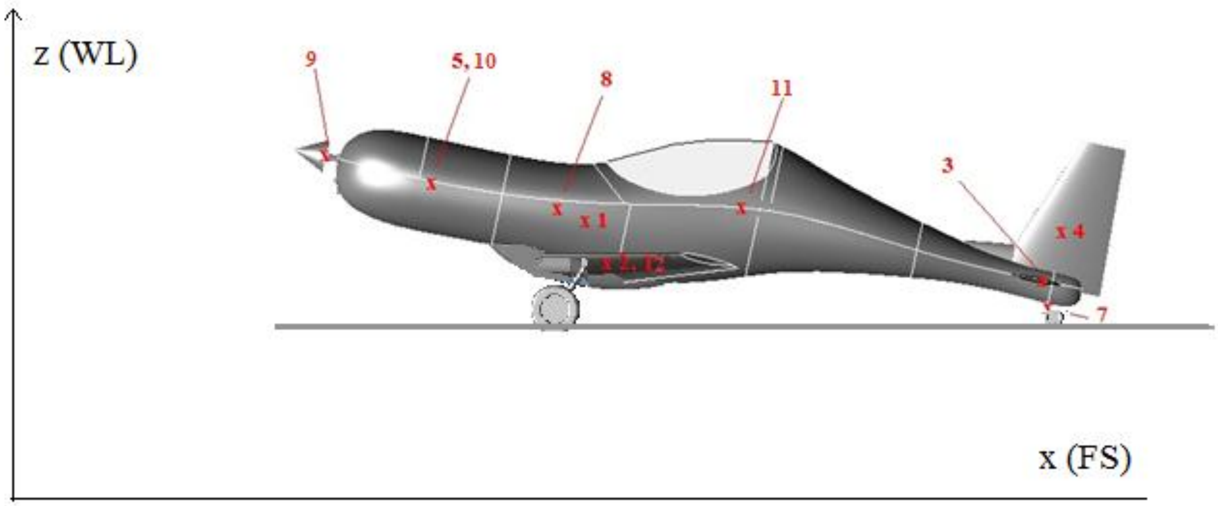


**Figure 6.2: Component Center of Gravity Locations**

Since the Renosaur is symmetric, the z- and x-coordinates define the center of gravity for each component. The c.g. locations are either determined with the methods shown in Table 10.2, Ref. 5, or estimated using engineering judgment. The following three loading cases are evaluated:

- Loading Case 1: Maximum takeoff weight with race fuel
- Loading Case 1: Maximum takeoff weight with 50% of race fuel
- Loading Case 3: Maximum takeoff weight with ferry fuel

The c.g. locations for Loading Case 1 are listed in Table 6.4.

**Table 6.4: Class II Weight and Balance Calculation**

| | Component | Weight fraction (~) | Weight (lbf) | FS (in) | WL (in) | Wx (in-lbf) | Wz (in-lbf) |
|---|---|---|---|---|---|---|---|
| 1 | Fuselage group | 0.155 | 800 | 800.0 | 172 | 81 | 137600 |
| 2 | Wing group | 0.155 | 800 | 800.0 | 174 | 74 | 139200 |
| 3 | Horizontal tail | 0.021 | 110 | 110.0 | 304 | 64 | 33440 |
| 4 | Vertical tail | 0.015 | 80 | 80.0 | 310 | 76 | 24800 |
| 5 | Engine group | 0.206 | 1065 | 1065.0 | 133 | 95 | 141645 |
| 6 | Main gear | 0.066 | 340 | 340.0 | 154 | 62 | 52360 |
| 7 | Rear gear | 0.015 | 76 | 76.0 | 307 | 56 | 23332 |
| 8 | Fixed equipment group | 0.213 | 1103 | 1103.0 | 209 | 72.8 | 230527 |
| 9 | Propeller group | 0.092 | 477 | 477.0 | 97 | 102 | 46269 |
| **Empty weight** | | | | | | | |
| 10 | Trapped fuel and oil | 0.005 | 26 | 133 | 95 | 3445 | 2461 |
| 11 | Crew | 0.039 | 200 | 219 | 86 | 43800 | 17200 |
| **Operative empty weight** | | | | | | | |
| 12 | Fuel | 0.019 | 98 | 177 | 69 | 17258 | 6728 |
| | **Total** | **1** | **5175** | | | | |

The center of gravity locations for the three loading cases are listed in Table 6.5.

**Table 6.5: Center of Gravity locations**

| | $x_{cg}$ (in) | $y_{cg}$ (in) | $z_{cg}$ (in) |
|---|---|---|---|
| **Loading Case 1** | | | |
| $W_E$ | 173.0 | 0 | 79.7 |
| $W_{OE}$ | 174.6 | 0 | 80.1 |
| $W_{TO}$ | 174.7 | 0 | 79.8 |
| **Loading Case 2** | | | |
| $W_E$ | 173.0 | 0 | 79.7 |
| $W_{OE}$ | 174.6 | 0 | 80.1 |
| $W_{TO}$ | 174.6 | 0 | 79.9 |
| **Loading Case 3** | | | |
| $W_E$ | 173.0 | 0 | 79.7 |
| $W_{OE}$ | 174.6 | 0 | 80.1 |
| $W_{TO}$ | 174.8 | 0 | 79.2 |

The data presented in Table 6.5 is used to construct the center of gravity excursion plot. This plot is presented in Figure 6.3.

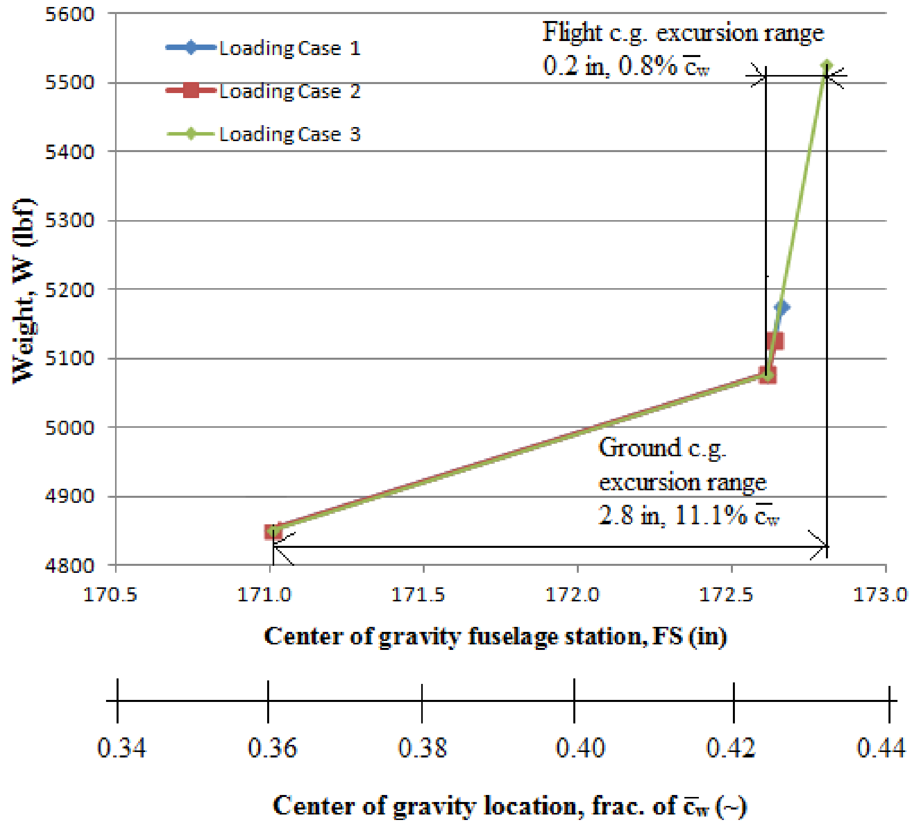


**Figure 6.3: Center of Gravity Excursion Diagram**

The most forward and aft positions of the center of gravity are as follows:

- Most forward: FS 170.9 in
- Most aft: FS 172.7 in

These values correspond to an 11.1 % of the mean geometric chord shift in c.g. on the ground and a 0.8 % of the mean geometric chord shift in c.g. in flight. This assumed to be an acceptable c.g. excursion.

# 7 CLASS II DRAG BUILD-UPS & DRAG POLARS

The Class II drag polars and drag build-ups are presented in this Section. The method followed in this Section is based on Ref. 9.

## 7.1 CLASS II DRAG POLARS

To determine the Class I drag polars, the wetted area of the Renosaur needs to be determined.

### 7.1.1 WETTED AREA DETERMINATION

To analyze the drag polars the wetted area of all components of the Renosaur need to be determined.

The fuselage, wing and empennage are the main contributors to the total wetted area.

The wetted area of the fuselage is determined with a perimeter plot, which can be found in Figure 7.1.

The different fuselage cross sections and the corresponding fuselage stations are presented.

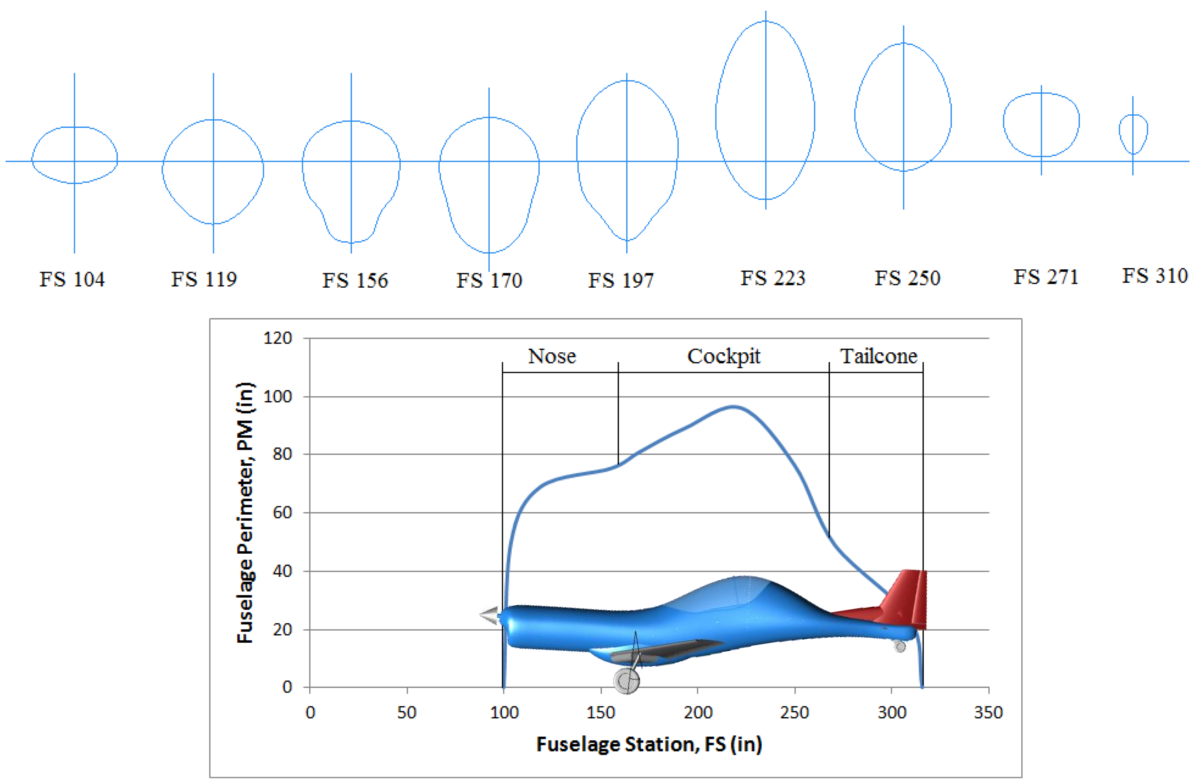


**Figure 7.1: Fuselage Cross Sections and Perimeter Plot**

Furthermore, the wetted area of the fuselage is determined in Shark FX and with the method presented in Ref. 5. The fuselage wetted areas are given in Table 7.1.

**Table 7.1: Fuselage Wetted Areas**

| Perimeter plot | CAD | Ref. 5 |
|---|---|---|
| 101.4 $ft^2$ | 98.5 $ft^2$ | 90.0 $ft^2$ |

The wetted area of the wing and the empennage surfaces is determined from the CAD model and determined with the method presented in Ref. 5. The wetted areas for the different components of the Renosaur are presented in Table 7.2.

**Table 7.2: Wing and Empennage Wetted Areas**

| | CAD | Ref. 5 | Difference |
|---|---|---|---|
| Wing | 74.3 $ft^2$ | 70.7 $ft^2$ | 5.1 % |
| Horizontal tail | 9.3 $ft^2$ | 8.7 $ft^2$ | 6.9 % |
| Vertical tail | 8.1 $ft^2$ | 7.0 $ft^2$ | 15.7 % |

The total wetted area is the sum of the wetted areas determined from the CAD model and is as follows:

- $S_{wet} = 191\ ft^2$

The total wetted area is compared with the values in Figure 3.22a, Ref. 5. An average wetted area for single and twin engine propeller driven aircraft is 900 $ft^2$. This is significantly higher than the value determined for the Renosaur. This is due to the high wing loading and small wing area of the Renosaur.

### 7.1.2 DRAG POLAR ANALYSIS

In this Section the Class II drag polars for cruise, takeoff and landing are determined. The equivalent parasite area, f, is found from Fig. 3.21, Ref. 5 for a wetted area of 191 $ft^2$. The following skin friction coefficient and equivalent parasite area are selected:

- $c_f = 0.0030$
- $f = 1.0\ ft^2$

The zero lift drag coefficient, $C_{D0}$, is determined to be 0.0245.

The Renosaur is flying in the race at a Mach number of 0.79. This results in an estimated compressibility drag increment of 0.003, assuming the Renosaur is designed as clean as a Boeing 727 (Fig. 12.7, Ref. 4). Next the landing gear increments are determined using Table 3.6, Ref. 5. Since the Renosaur does not need flaps, no drag increments will result from that. The drag increment and Oswald's efficiency factor are presented in Table 7.3. Finally, the drag polars of the Renosaur are determined. The drag polars are presented in Table 7.4.

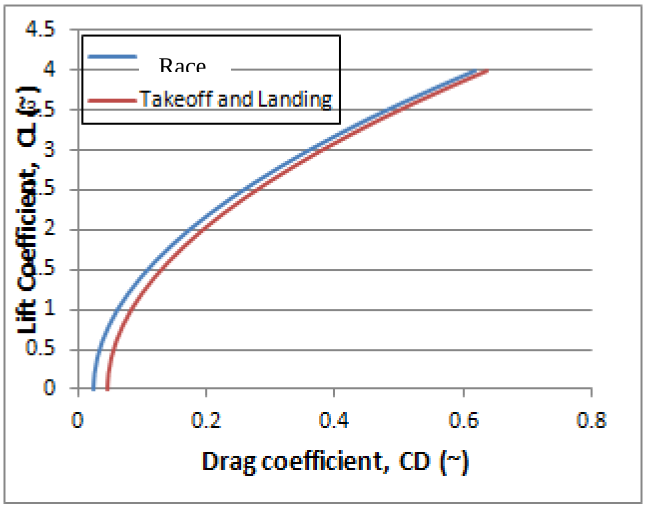


**Figure 8.2: Class I Drag Polars**

**Table 7.3: Drag increments**

| | $\Delta C_{D_o}$ | e |
|---|---|---|
| Race | 0 | 0.85 |
| Landing gear | 0.02 | no effect |

**Table 7.4: Class II Drag Polars**

| | **Drag Polars** |
|---|---|
| Race | $C_D = 0.0248 + 0.037C_L^2$ |
| Takeoff | $C_D = 0.0448 + 0.037C_L^2$ |
| Landing | $C_D = 0.0448 + 0.037C_L^2$ |

## 7.2 IMPACT OF L/D ANALYSIS ON DESIGN

The lift-to-drag ratios for the Renosaur are given in Table 7.5.

**Table 7.5: L/D ratios**

| | **L/D values calculated** | **L/D values assumed** |
|---|---|---|
| $(L/D)_{cruise}$ | 6.4 | 7.0 |
| $(L/D)_{TO}$ | 11.4 | 10.0 |
| $(L/D)_L$ | 11.2 | 10.0 |

As can be seen in Table 7.5, the calculated L/D values differ from the assumed values. The change in takeoff weight can be determined by using Equation 7.1.

$$\Delta W_{TO} = \Delta\left(\frac{L}{D}\right)\left(\frac{\partial W_{TO}}{\partial \frac{L}{D}}\right) \qquad \text{(Equation 7.1)}$$

The takeoff weight sensitivity with respect to L/D is determined in Section 3 to be -10 lbf. The changes in takeoff weight due to the change in L/D are presented in Table 7.6. These changes are negligible with respect to the 5175 lbf takeoff weight. The largest change in takeoff weight is a 0.30 % increase in takeoff weight. Since the weight does not change more than 5 %, resizing of the Renosaur is not necessary (Ref. 5).

**Table 7.6: Change in takeoff weight**

| | |
|---|---|
| Cruise | 15.9 lbf increase |
| Takeoff | 14.0 lbf decrease |
| Landing | 11.8 lbf decrease |

7.3 <u>CLASS II DRAG BUILD-UPS & DRAG POLARS</u>

This Section documents the Class II drag build-up. The Class II drag build-up is presented in Figure 7.3.

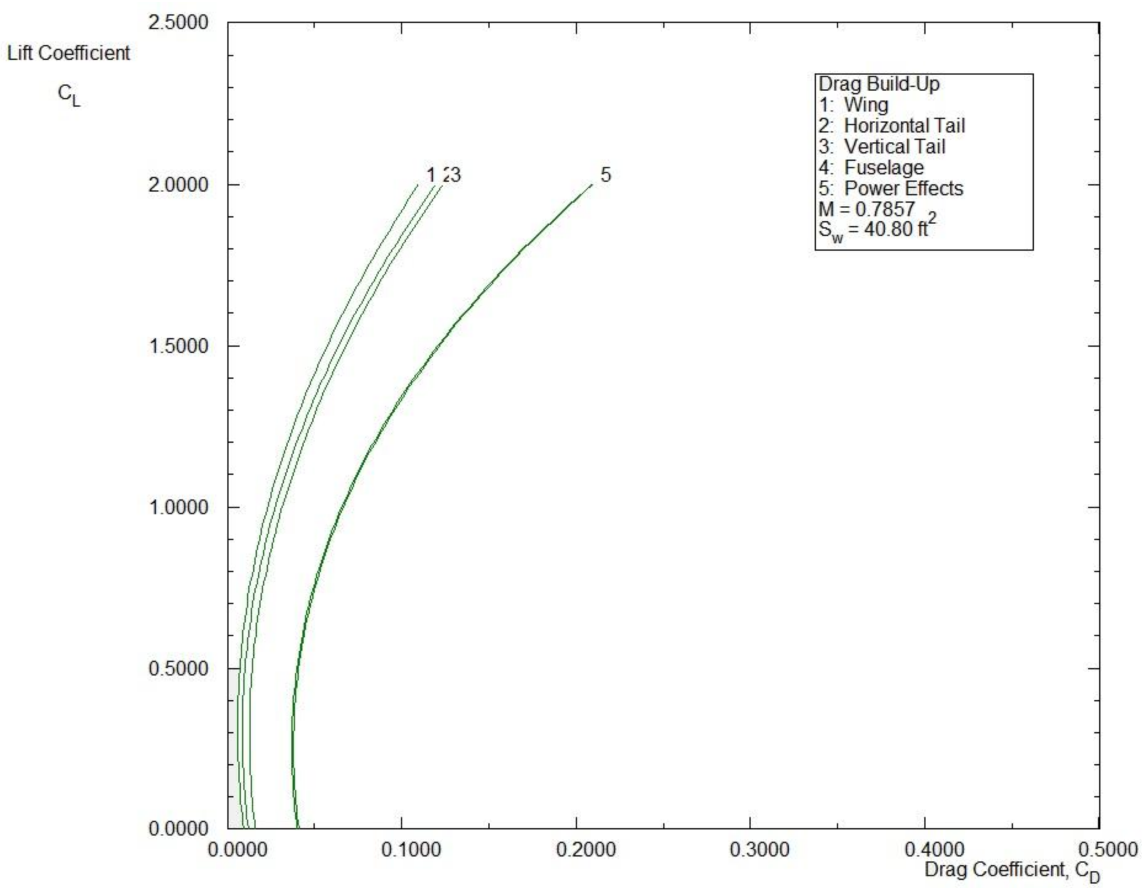


**Figure 7.3: Class II Drag Build-Up**

# 8 CLASS II PROPULSION PERFORMANCE

This Section presents the Class II propulsion performance. The specifications of the engine installation are given and the risks in selecting this configuration are considered.

## 8.1 ENGINE SPECIFICATIONS

The engine used on the Renosaur is the BMW P84/5 engine. The specifications are given in Table 8.1 and the engine is presented in Figure 8.1.

**Table 8.1: BMW P84/5 Specs (Ref. 19)**

| | |
|---|---|
| Engine type | BMW P84/5 V10 |
| Cylinders | 10 |
| Bank angle | 90 deg |
| Displacement | 2998 cc |
| Weight | 203 lbf |
| Height | 12.6 in |
| Width | 21.06 in |
| Length | 22.78 in |
| Brake horsepower | 925 bhp |
| Fuel consumption | 2.94 mpg |
| Engine speed | 19,000 rpm |

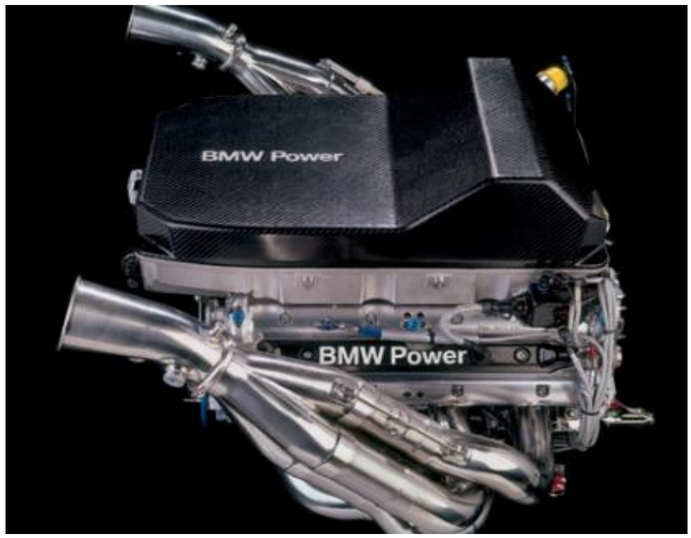


**Figure 8.1: BMW P84/5 engine (Ref. 19)**

## 8.2 ENGINE PERFORMANCE AND MATERIALS

The BMW P84/5 engine has a power-to-weight ratio of 4.6 hp/lbf, where the power-to-weight ratio of a Pratt & Whitney R-2800 equals 0.89 hp/lbf. This is a significant increase and a great advantage over the engines used in Unlimited Class racers currently. The materials used for the production of the BMW P84/5 engine are summarized in Table 8.2. The casting quality of the engine block and the cylinder head play a crucial role in the performance and endurance of the engine.

**Table 8.2: Engine materials and systems (Ref. 19)**

| | |
|---|---|
| Cylinders | Four valves per cylinder |
| Valve drive | Pneumatic |
| Engine block | Aluminum |
| Cylinder head | Aluminum |
| Crankshaft | Steel |
| Oil system | Dry sump lubrication |

## 8.3 ENGINE SELECTION RISKS

There are a number of risks involved in selecting a Formula One engine for the Renosaur. The main challenges are the following:

- Formula One engines are designed for use in race cars, their behavior in aircraft is unknown;
- The engine rpm of 19,000 rpm is too high for use in aircraft, therefore a gear reduction is needed;
- There is very limited data available on these engines, because manufacturers do not publish detailed engine specifications;
- The endurance of the engine is unknown. A short lifetime might increase the airplane cost significantly;
- The engine cost is not published; in the cost analysis (Section 13) an initial value of $300,000 is assumed.

# 9 CLASS II STABILITY AND CONTROL

The purpose of this Section is to determine the stability and control characteristics of the Renosaur. The static longitudinal and directional stabilities are determined. Furthermore, trim diagrams for different flying conditions are provided.

## 9.1 STATIC LONGITUDINAL STABILITY

The longitudinal X-plot for the Renosaur is presented in Figure 9.1. In the X-plot the horizontal tail area is desired for a desired static margin.

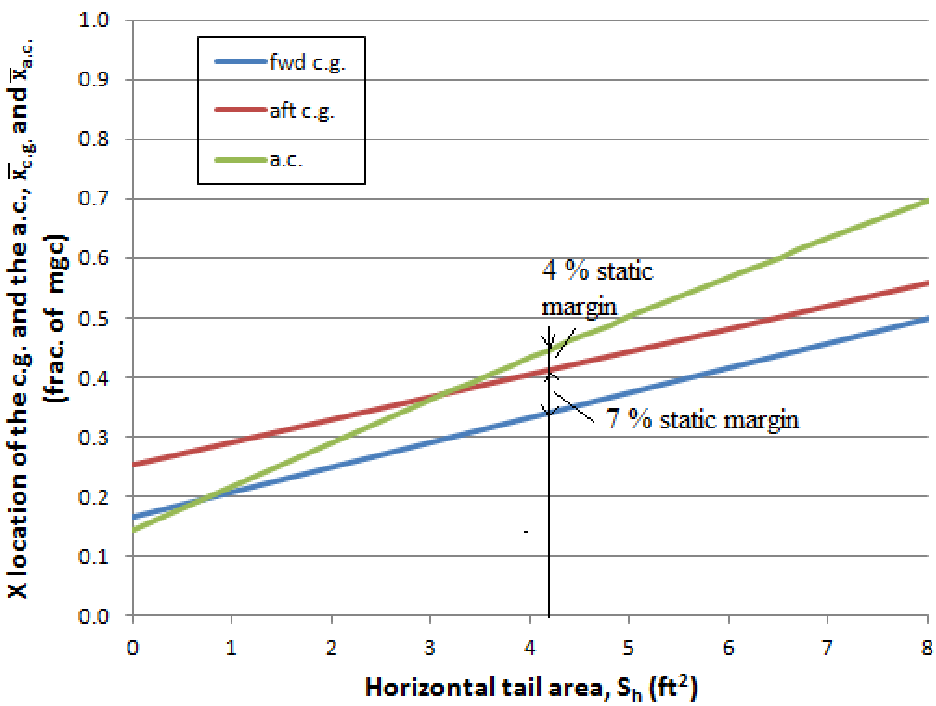


**Figure 9.1: Longitudinal X-plot for the Renosaur**

The Renosaur needs to be inherently stable. This decision is made for the following reasons:

- The use of a stability augmentation system increases the cost of the Renosaur significantly;
- If the FAA decides to force regulations on Reno racers, it is likely that inherent stability is a requirement.

A static margin of 4 % is selected for the Renosaur. This value is chosen to design for maximum maneuverability. The author assumes the pilot will be comfortable with flying an aircraft with a low static margin.

From Figure 9.1 the following values are determined:

- Static margin = 4.0 %
- Center of gravity travel = 6.9 %
- Maximum static margin = 10.9 %

The horizontal tail area is determined from the longitudinal X-plot. This value is compared with the value obtained from the volume coefficient method. The horizontal tail areas are as follows:

- Longitudinal X-plot: $S_h$ = 4.2 %
- Volume coefficient method: $S_h$ = 5.9 %
- Difference = 28.8 %

It is desirable to keep the change in tail size within 20 %. The difference is slightly larger with 28.8 %, but still within acceptable bounds in the opinion of the author.

## 9.2 STATIC DIRECTIONAL STABILITY

In this Section the static directional stability is determined by creating a directional X-plot. The yawing moment coefficient due to sideslip is determined as a function of vertical tail area.

The directional X-plot for the Renosaur can be seen in Figure 9.2.

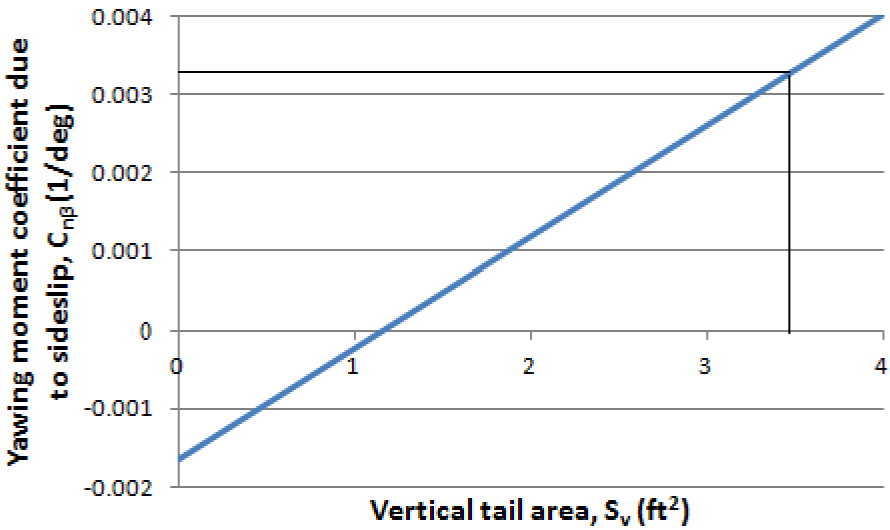


**Figure 9.2: Directional X-plot**

Since the Renosaur is an inherently stable aircraft, the yawing moment due to sideslip is set to a minimum of 0.0010 per degree (Eq. 11.9, Ref. 6). However, since this method decreased the tail size too much, the vertical tail size that has been determined with the volume coefficient method is used. The resulting yawing moment due to sideslip is equal to 0.0032 per degree. The vertical tail size of 3.4 $ft^2$ determined with the volume coefficient method is maintained

## 9.3 CLASS II STABILITY & CONTROL

The objectives of the Class II Stability & Control analysis are to assure that:

- the airplane has sufficient control power to maintain steady state, straight line flight
- the airplane can be safely maneuvered from one steady state flight condition to another
- cockpit control force levers are acceptable under all expected conditions, including those caused by configuration changes
- the airplane can be trimmed in certain flight conditions

To determine the Class II Stability and Control, a trim diagram is computed. The trim diagram shows the relation between the lift coefficient and pitching moment coefficient and the lift coefficient and the angle of attack. AAA is used to determine the trim diagrams. The trim bucket is the area enclosed by the forward and aft c.g. and the maximum angle of attack. The trim diagram for the Renosaur is shown for the conditions presented in Table 9.1.

**Table 9.1: Trim diagram conditions**

| Condition | Load factor |
|---|---|
| Race | 3.5 g |
| Race | 1 g |
| Landing | 1 g |
| Takeoff | 1 g |

To get a reasonable trim diagram the center of gravity of the aircraft needed to be shifted back 0.5 feet. The trim diagrams are presented in Figure 9.3 to 9.6. AAA screenshots of the inputs for the race trim diagrams are provided in Appendix A.

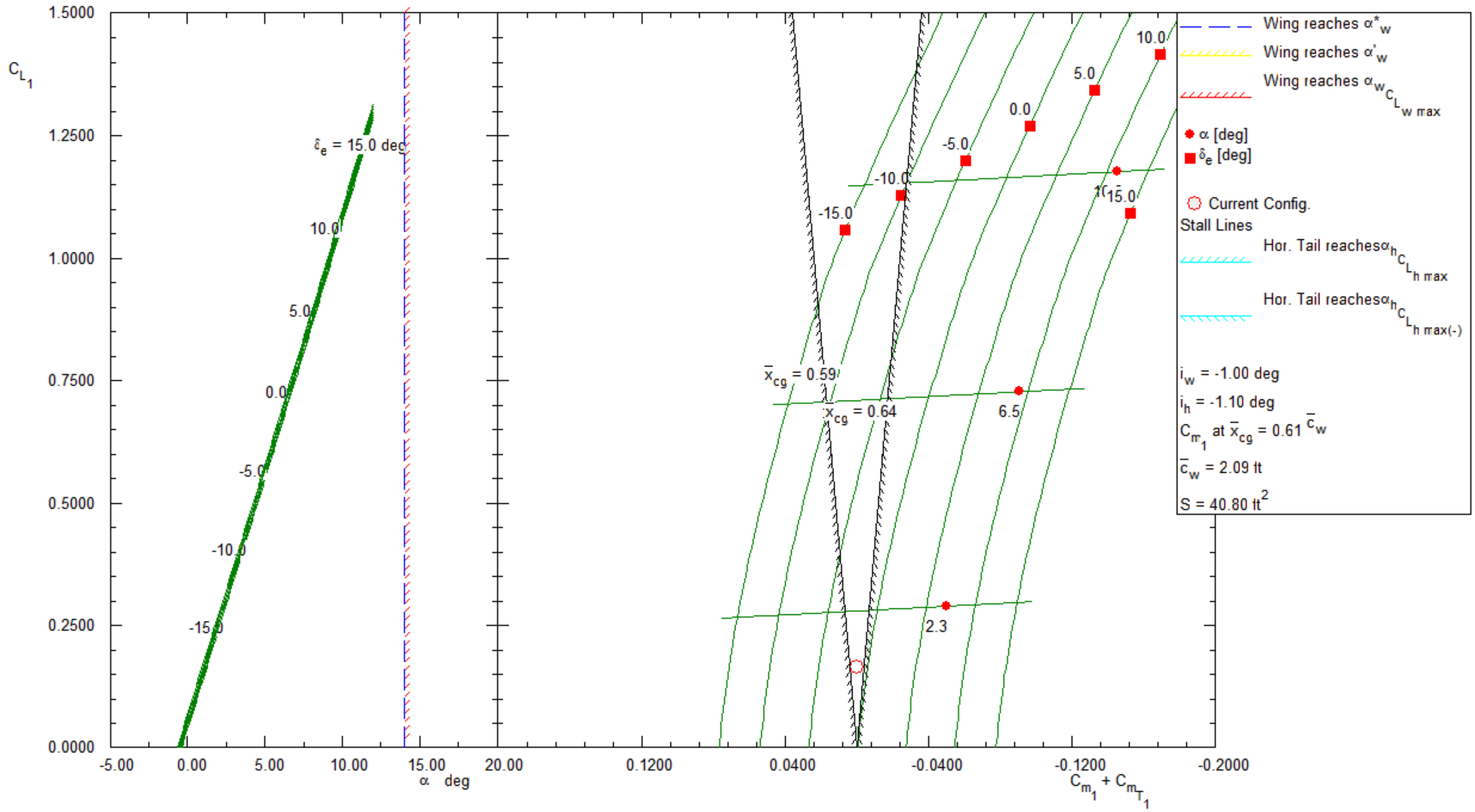


**Figure 9.3: Trim diagram for the Renosaur during race conditions in 1 g flight**

The trim diagram in the race in a 3.5 g turn is presented in Figure 9.4. The trim diagrams for takeoff and landing during 1 g flight are presented in Figure 9.5 and Figure 9.6, respectively.

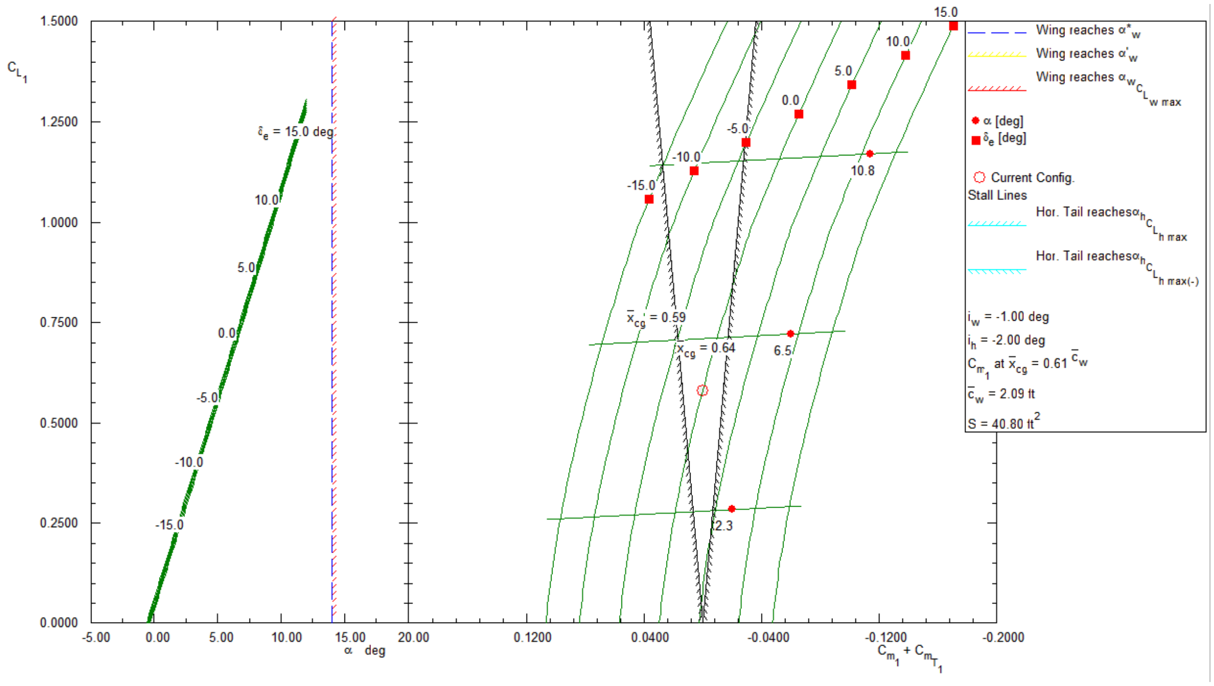


**Figure 9.4: Trim diagram for the Renosaur in race conditions in a 3.5 g turn**

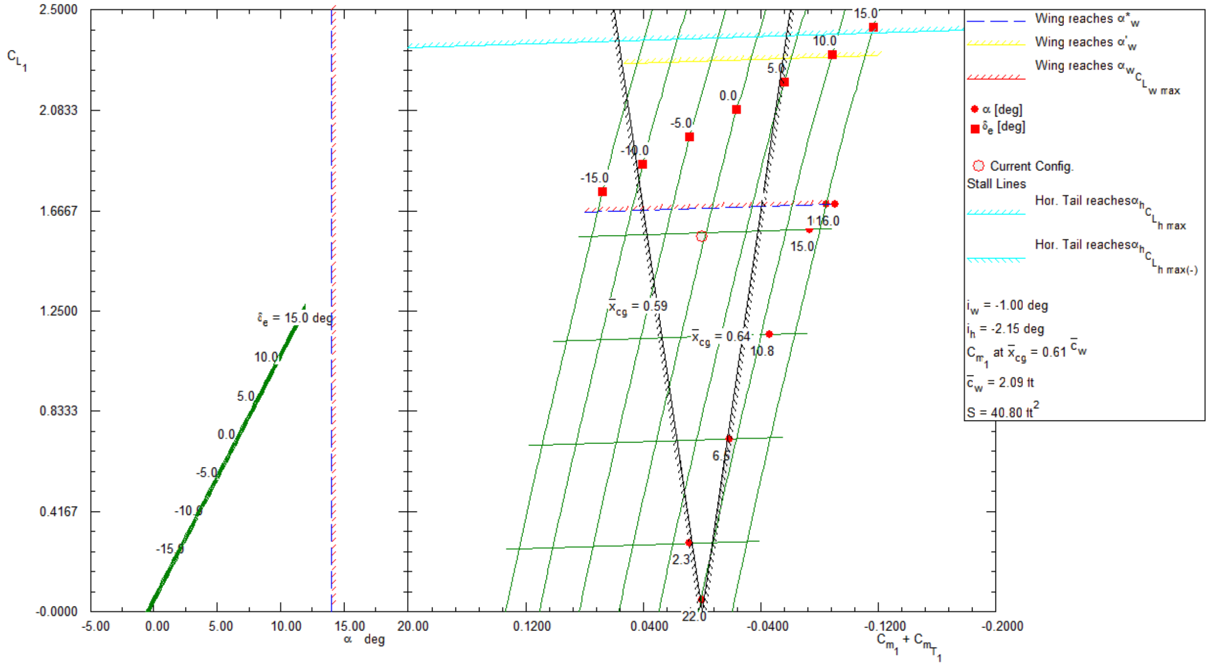


**Figure 9.5: Trim diagram for the Renosaur during landing in 1 g flight**

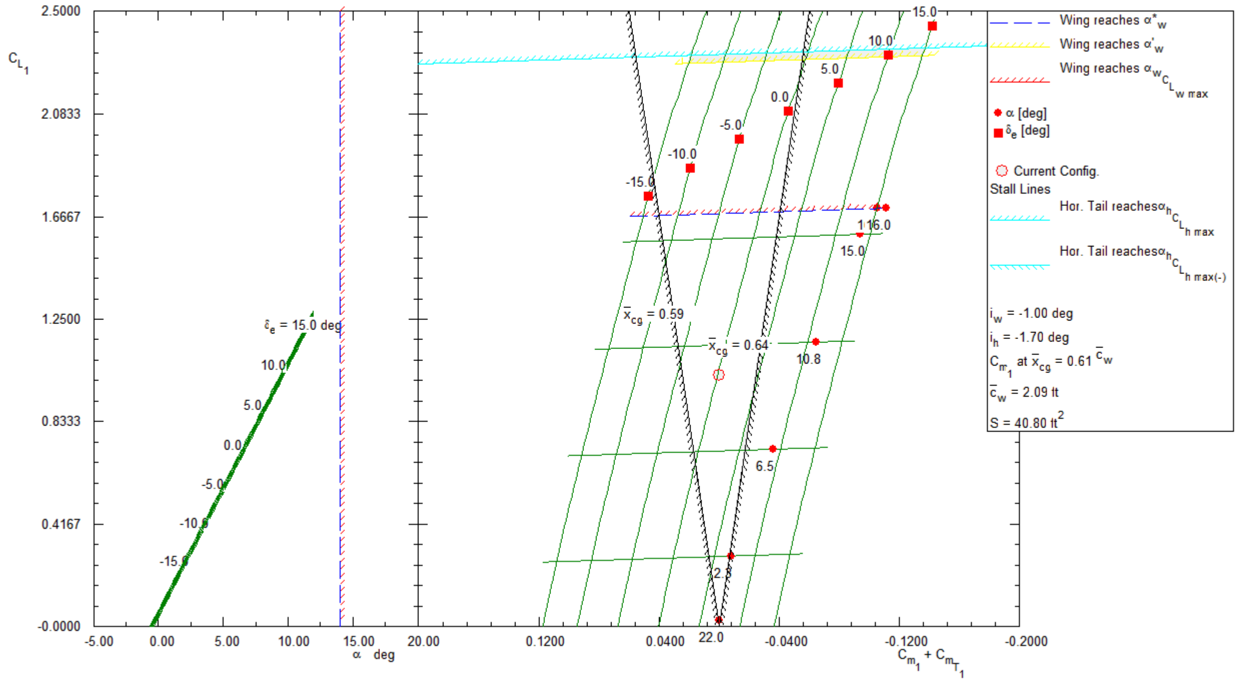


**Figure 9.6: Trim diagram for the Renosaur during takeoff in 1 g flight**

# 10 STRUCTURES

This Section presents the structural layout of the Renosaur as well as the materials and manufacturing techniques used. At this stage only simplified CAD drawings of the Renosaur are made, since the author is going to make a new CAD model in CATIA.

## 10.1 LAYOUT OF STRUCTURAL COMPONENTS

### 10.1.1 Fuselage

The fuselage skin will be constructed from graphite. The fuselage is a fully monocoque structure and will be manufactured in two parts: the left side and the right side of the fuselage. The fuselage will be manufactured around a silicon plug with four moulds. This will result in a seamless fuselage. The fuselage skin is positioned around the forward and aft bulkhead, to allow for additional strength.

### 10.1.2 Wing

The wing of the Renosaur will be constructed using graphite and reinforced with tungsten around the leading edge. The wing will be produced with half-wing casting, resulting in two half-wing structures, joined in the middle with a doubler. This half-wing casting process consists of the graphite structure, with silicone within and plugs in the silicon. These plugs will be inflated to approximately 180 psi, pushing the graphite structure against a top and bottom mould, which are joined with bolts. The mould will be produced from invar or casting graphite, to minimize the thermal expansion. At the end of the process the plugs will be pulled out of the structure by applying vacuum, and a solid, graphite structure will remain.

### 10.1.3 Empennage

The empennage is constructed in a similar way as the main wing. The empennage is constructed of graphite, and the vertical tail and horizontal tail are manufactured as a whole with the casting process described in Section 10.1.2.

### 10.1.4 Landing Gear Integration

The landing gear is integrated in the wing-fuselage structure. Structural synergism is used by attaching the landing gear to the front spar of the wing.

## 10.2 CAD DRAWINGS OF STRUCTURAL LAYOUT

Since the fuselage is a fully monocoque structure, no additional stiffeners need to be made in CAD. In a similar way, the wing will be produced in two pieces, where no ribs or stiffeners are needed. A general layout of the structural layout can be seen in Figure 10.1.

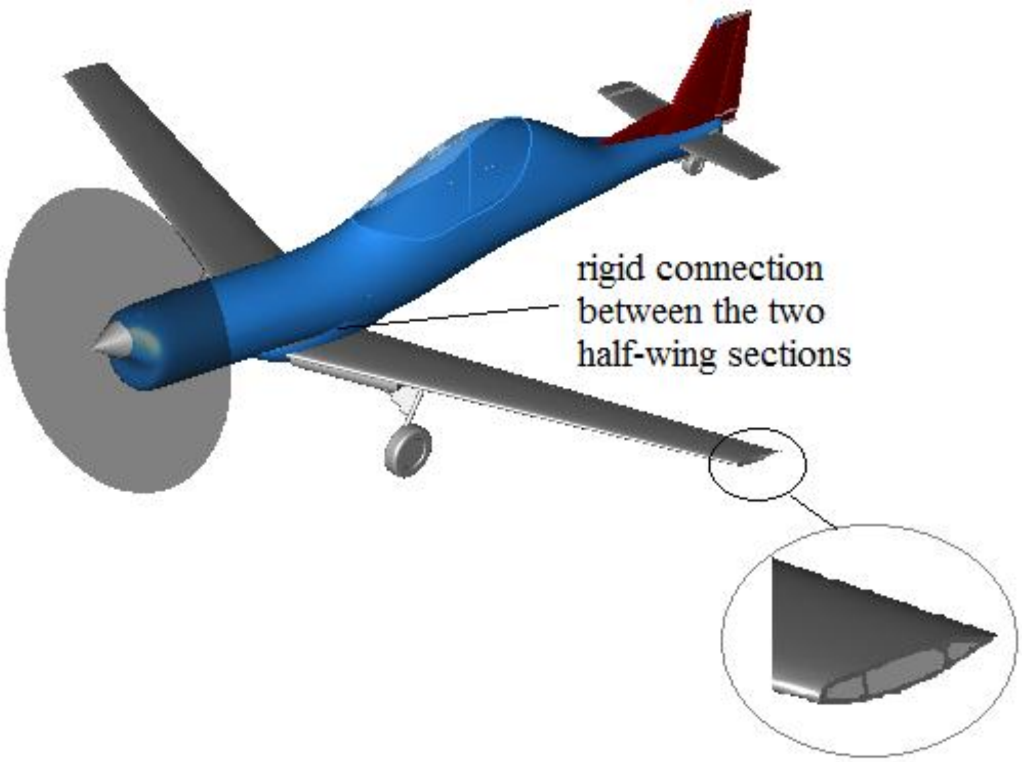


**Figure 10.1: Structural layout of the Renosaur**

A simplified exploded view of the Renosaur is presented in Figure 10.2. A more detailed CAD drawing will be made when the author has modeled the aircraft in CATIA.

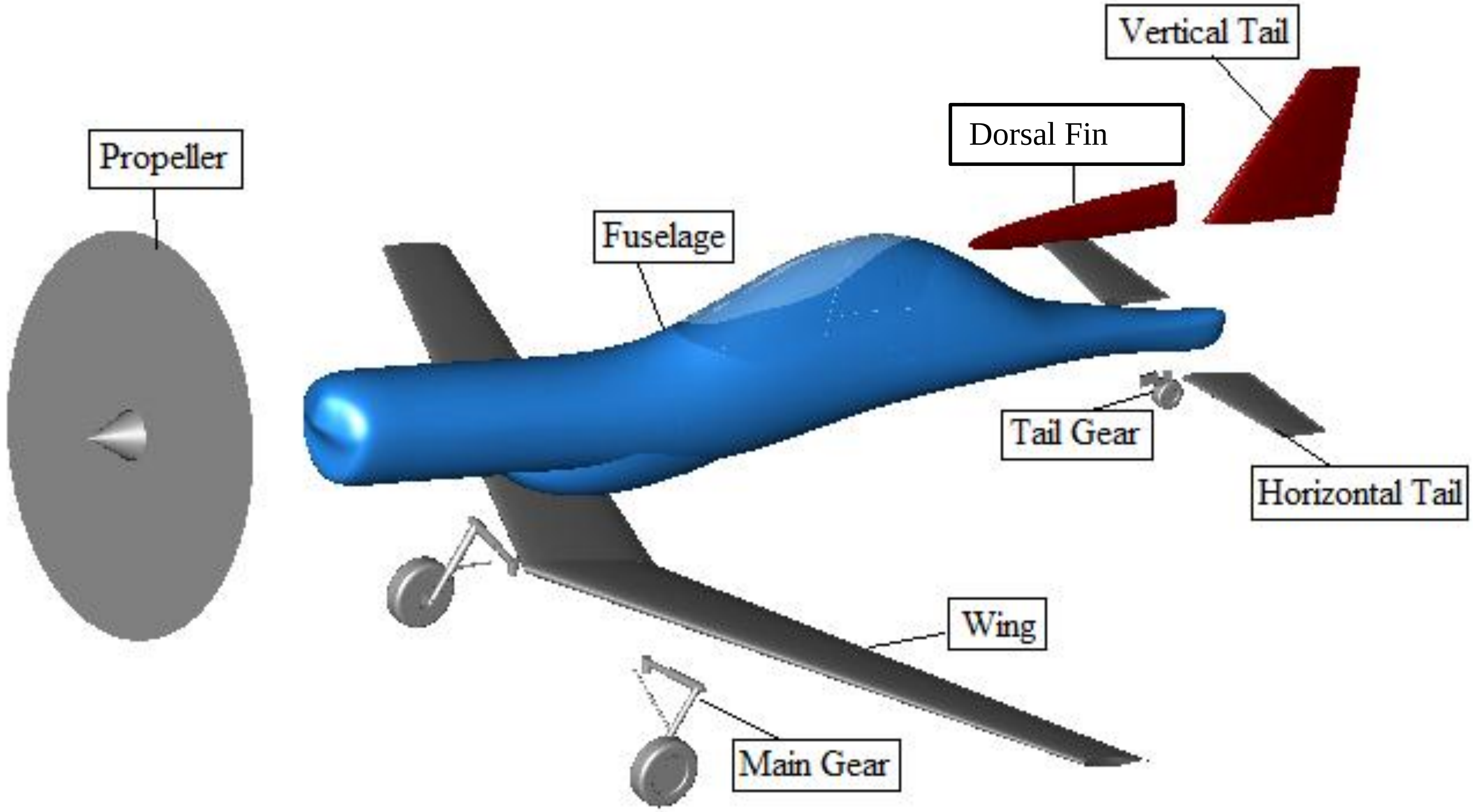


**Figure 10.2: Exploded View of the Renosaur**

# 11 SYSTEMS

This Section documents the description of the major systems with ghost views. The procedures followed in this Section are based on the method shown in Ref. 7. The reasons for identifying the required airplane systems are (Ref. 7):

- Airplane systems have a significant impact on the empty weight
- To determine any obvious conflicts which would arise by having two or more systems occupy the same space occupied in the airplane

The layouts of the flight control, fuel, electrical and hydraulic systems are presented in this Section.

## 11.1 DESCRIPTION OF THE FLIGHT CONTROL SYSTEM

The flight control system of the Renosaur is selected to be irreversible with fly by wire controls. This system has the following advantages:

- Lightweight
- Responsive
- Easier to include redundancy

The flight control system will be driven by electrohydrostatic (EHS) actuators. This actuator does not require an airplane hydraulic system, since EHS actuators have their own miniature hydraulic system including a pump and an electric motor which drives the pump. An advantage of electrohydrostatic actuators is that there is no need for hydraulic lines to each control surface. A single electrical line is needed for each actuator (Pg. 236, Ref. 7). Triple redundancy is included for all primary flight control systems. The primary and secondary control systems of the Renosaur are given in Table 11.1.

**Table 11.1: Flight control systems**

| **Primary flight control systems** | **Secondary flight control systems** |
|---|---|
| Ailerons<br>Elevator<br>Rudder | Trim controls<br>Power controls |

### 11.1.1 Ailerons

The layout of the electrical lines running to the electrohydrostatic actuators used for the aileron controls can be seen in Figure 11.1. The electrical lines are either routed against the fuselage skin or against the aft bulkhead. The location of the actuators can be found on the top view. The actuator properties are given in Table 11.2. For the determination of the required control force, the hingemoment coefficient is determined in AAA.

**Table 11.2: Aileron Actuator Properties**

| | |
|---|---|
| Required control force, $F_c$ (lbf) | 1200 |
| Deflection rate (deg/sec) | 500 |
| Control Rod Velocity (in/sec) | 10.5 |

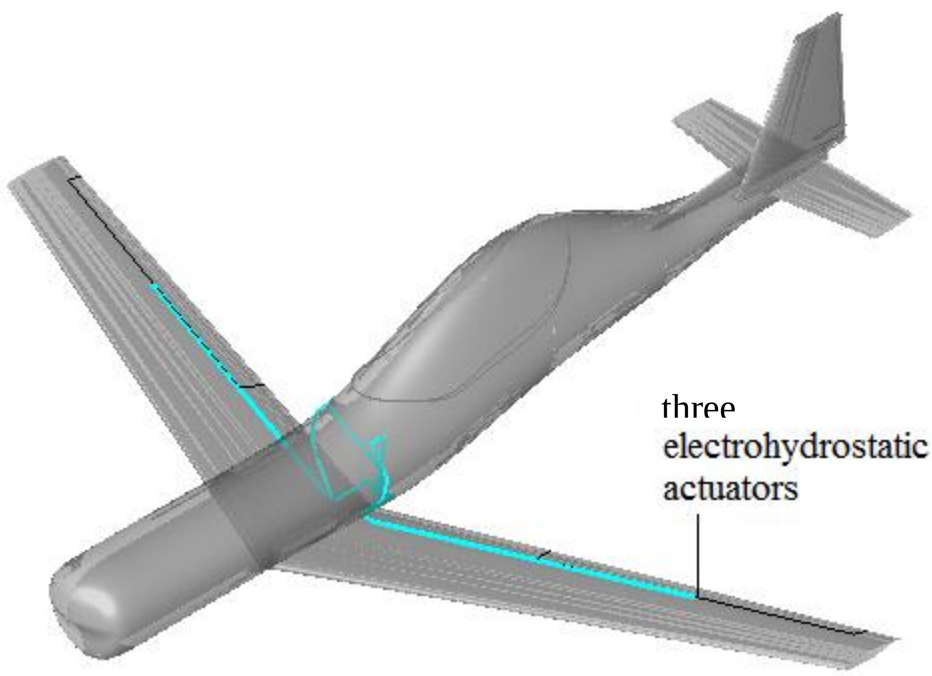


**Figure 11.1: Ghost View with Aileron Control System**

### 11.1.2 Elevator

The layout of the electrical lines running to the electrohydrostatic actuators used for the elevator controls can be seen in Figure 11.2. The electrical lines are either routed against the fuselage skin or against the aft bulkhead. The location of the actuators is indicated in the Figure. The actuator properties are given in Table 11.3.

**Table 11.3: Elevator Actuator Properties**

| | |
|---|---|
| Required control force, $F_c$ (lbf) | 1105 |
| Deflection rate (deg/sec) | 500 |
| Control Rod Velocity (in/sec) | 5.2 |

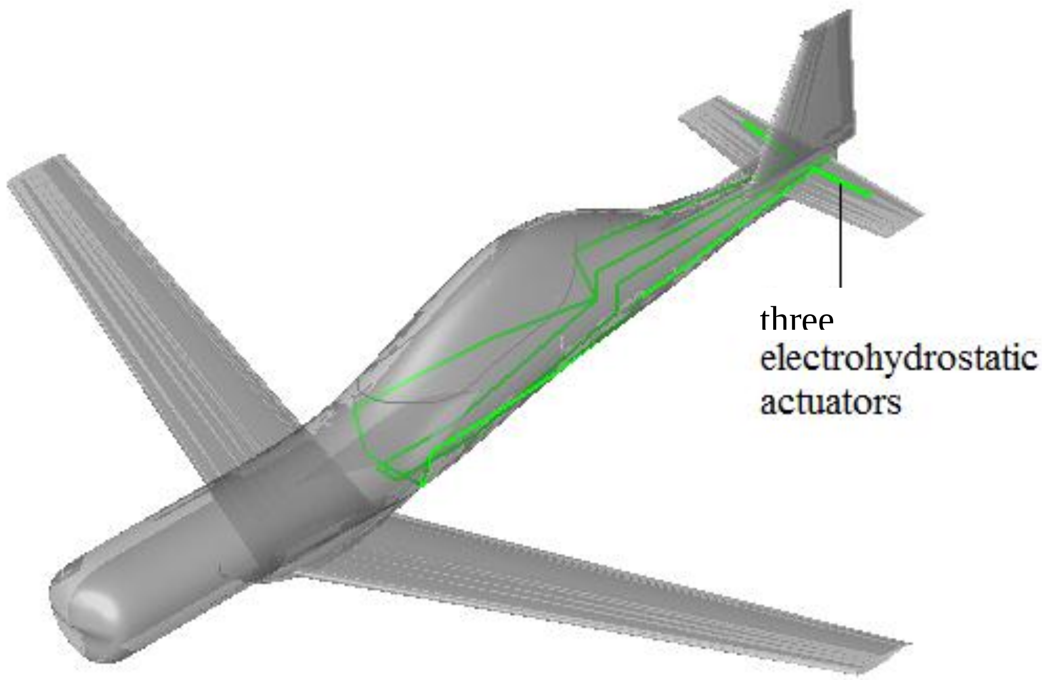


**Figure 11.2: Ghost View with Elevator Control System**

11.1.3 Rudder

The layout of the electrical lines running to the electrohydrostatic actuators used for the elevator controls can be seen in Figure 11.3. The electrical lines are either routed against the fuselage skin or against the aft bulkhead. The location of the actuators is indicated in the Figure. The actuator properties are given in Table 11.4.

**Table11.4: Rudder Actuator Properties**

| | |
|---|---|
| Required control force, $F_c$ (lbf) | 1521 |
| Deflection rate (deg/sec) | 500 |
| Control Rod Velocity (in/sec) | 4.2 |

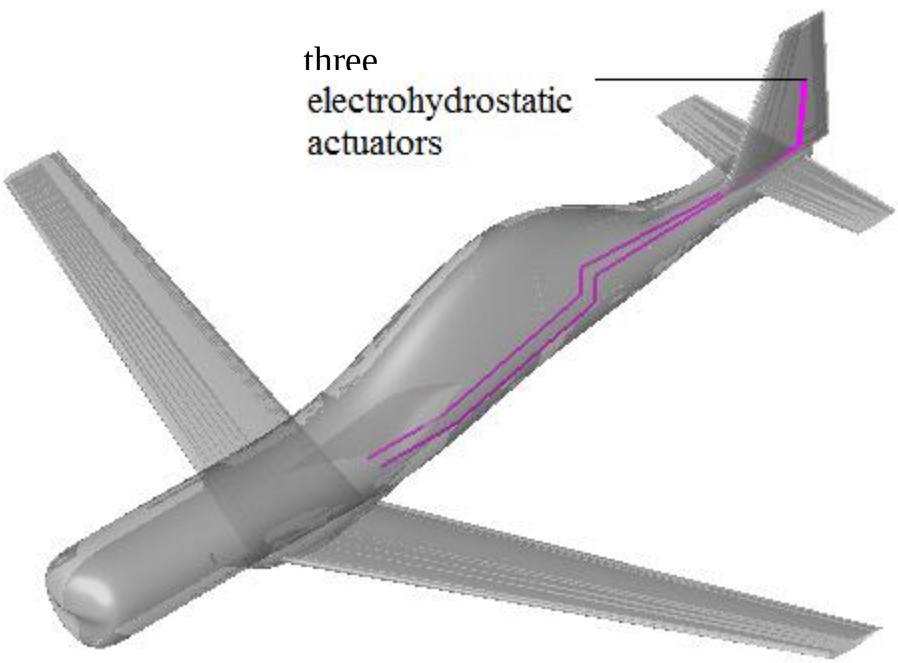


**Figure 11.3: Ghost View with the Rudder Control System**

11.1.4 Trim Controls

Ground adjustable trim tabs are installed on the Renosaur. In a later stage of the design process an irreversible trim control system will be added.

### 11.1.5 Power Controls

The power control system of the Renosaur consists of:

- Ignition control
- Starter system
- Throttle
- Mixture control

The starter is routed to the magneto of the engine and the throttle and mixture control are connected to the carburetor. This is all in a close distance from the engine and the lines will not be long. Therefore the author has decided CAD drawings will not be of additional value here.

## 11.2 DESCRIPTION OF THE FUEL SYSTEM

The fuel system of the Renosaur consists of:

- Fuel tanks
- Fuel pumps and fuel lines
- Fuel venting system
- Fuel quantity indicating system

The layout of the fuel system for the Renosaur can be seen in Figure 11.4. The two fuel tanks are positioned in the main wing. Since the Renosaur is a low wing aircraft, fuel pumps are needed to send the fuel to the engine. The required engine fuel flow is determined by multiplying the maximum required thrust by the associated fuel consumption, as can be seen in Equation 11.1.

$$Max. Fuel\ Flow = P_{TO}(c_p) \qquad \text{(Equation 11.1) (Equation 5.2, Ref. 8)}$$

The takeoff power is set to be 1732 hp and the specific fuel consumption is assumed in the preliminary sizing process to be 0.4 lbf/hp-hr. The maximum fuel flow is determined to be the following:

$$Max. Fuel\ Flow = 5175\ lbf\left(0.40\frac{lbf}{hp-hr}\right) = 866\frac{lbf}{hr}$$

The fuel volume is determined in Section 4 to be 4.43 ft$^3$. This is equal to 33.1 US gallons. The fuel pumps are located near the root of the wing, since the wing dihedral will cause the fuel to flow towards the root. Baffles are included to prevent the fuel from flowing away from the fuel pumps. Both fuel tanks are sealed with a self-sealing orifice. A fuel level indicator is included at the inboard station of the wing too.

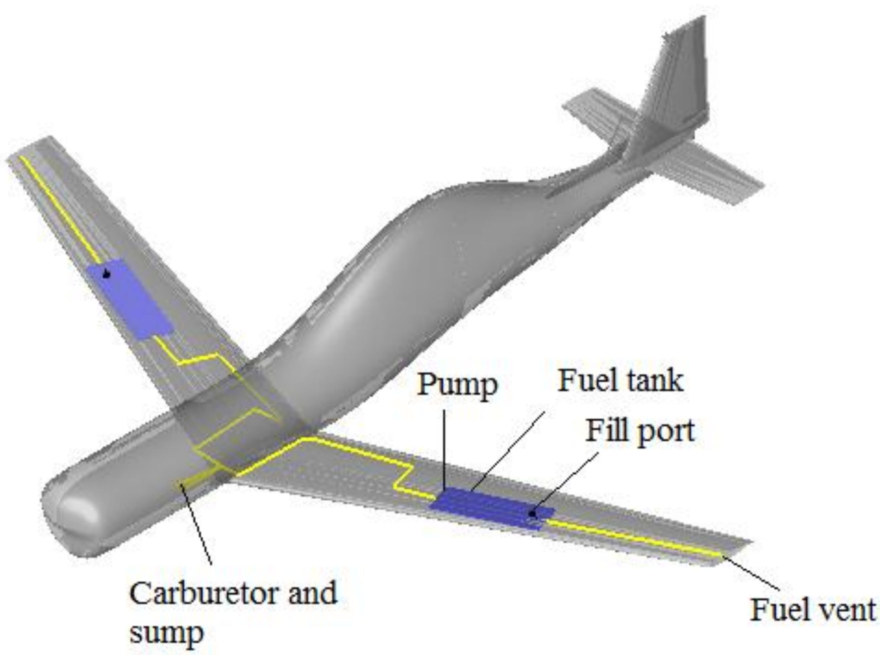


**Figure 11.4: Ghost View of the Fuel System**

## 11.3 DESCRIPTION OF THE ELECTRICAL SYSTEM

The electrical system for the Renosaur is shown in Figure 11.5. The electrical system is powered by batteries. Electrical load summaries are provided for ground loading, takeoff and climb and cruise. These can be found in Table 11.5, 11.6 and 11.7. Since the author was unable to find data on the power usage of the flight control actuators, initial values are assumed.

.

**Table 11.5: Ground Loading**

| | |
|---|---|
| Exterior lighting | 8 W |
| Flight compartment lighting | 2 W |
| Avionics | 12 W |
| Flight controls | 0 W |
| Total | 20 W |

**Table 11.6: Takeoff and Climb Loading**

| | |
|---|---|
| Exterior lighting | 8 W |
| Flight compartment lighting | 2 W |
| Avionics | 20 W |
| Flight controls | 40 W |
| Total | 70 W |

**Table 11.7: Cruise Loading**

| | |
|---|---|
| Exterior lighting | 6 W |
| Flight compartment lighting | 2 W |
| Avionics | 20 W |
| Flight controls | 30 W |
| Total | 60 W |

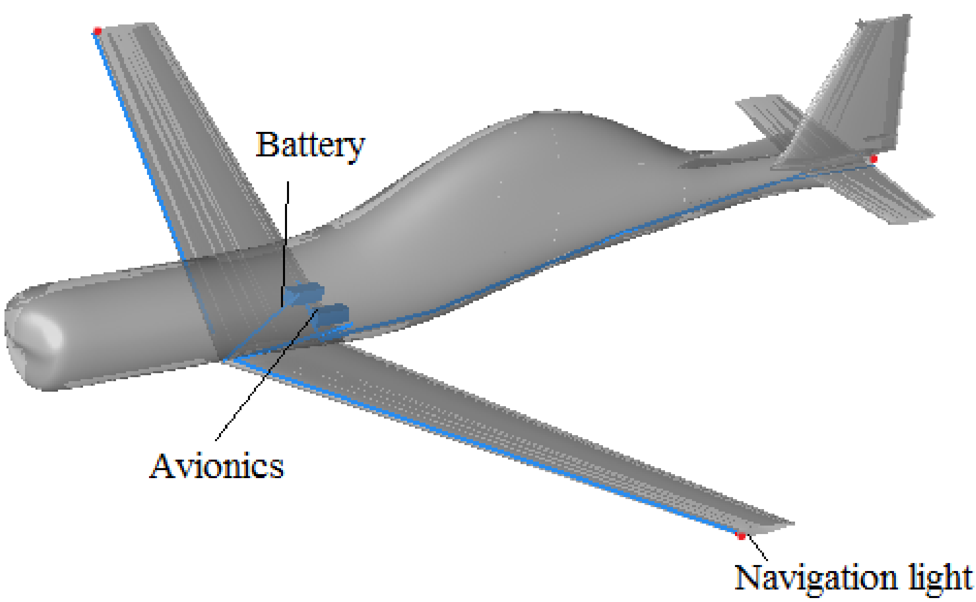


**Figure 11.5: Ghost View of the Electrical System**

## 11.4 DESCRIPTION OF THE HYDRAULIC SYSTEM

The hydraulic system is used to provide hydraulic power to actuators with the following tasks:

- Extending and retracting the landing gear
- Controlling wheel brakes
- Landing gear shock absorbers
- Operating thrust reversers

The hydraulic systems consist of the following components:

- Hydraulic fluid reservoir
- Hydraulic pumps
- Accumulators
- Fluid lines and valves

The hydraulic system layout for the Renosaur can be seen in Figure 11.6.

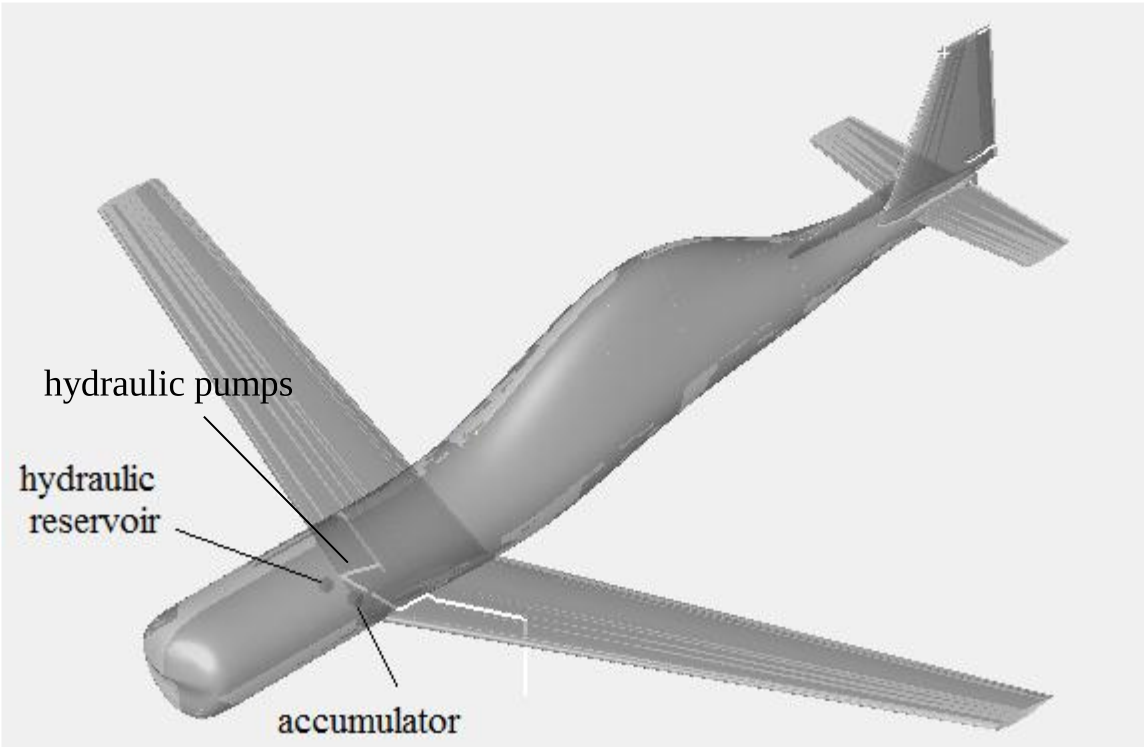


**Figure 11.6: Ghost View with Hydraulic System**

## 11.5 CONFLICT ANALYSIS

Two areas were conflicts can occur are in the tail cone and at the root of the wing. At the tail cone, a large number of lines are routed and interference may occur. Another problem section is the root of the wing. The landing gear is retracted in that section of the wing, and at the same time fuel lines and aileron control lines are routed there. The ghost view of all major systems is presented in Figure 11.7.

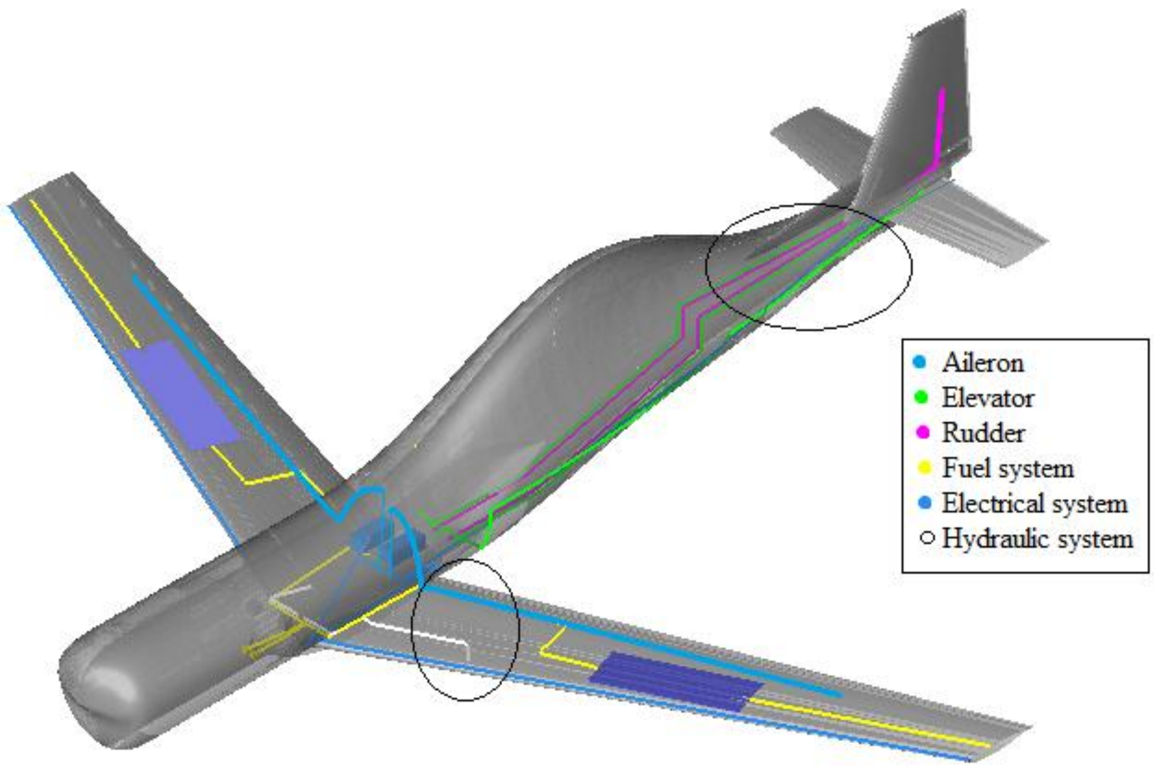


**Figure 11.7: Ghost View of All Major Systems**

# 12 ADVANCED TECHNOLOGIES

In this Section the advanced technologies used in the design process of the Renosaur are presented.

## 12.1 ADVANCED TECHNOLOGIES USED

The following advanced technologies are described in this Section:

- Fly-by-wire system with electrohydrostatic actuators
- Two in-line Formula One BMW P84/5 engines in combination with a TPE331 gear reduction
- Advanced materials: graphite and tungsten

### 12.1.1 Fly-by-wire flight control system

The first advanced technology used in the design of the Renosaur is the use of a fly-by-wire flight control system with electrohydrostatic actuators. Electrohydrostatic actuators are not widely used but assumed to be safe since double redundancy is incorporated. A fly-by-wire flight control system is selected to provide more flexibility in the command sequence. Furthermore, the fly-by-wire system has a lower weight than other flight control systems.

### 12.1.2 Formula One engines

Another advanced technology that is used is the engines of the Renosaur. The use of Formula One engines in air races is a new concept and the feasibility has yet to be proven. The combination of the two BMW P84/5 engines with the gear reduction of the TPE 331 is a risk in this design. However, the dimensions of the overall engine installation are significantly smaller in comparison with for example a Pratt & Whitney R2800. Also the weight of the engine installation is reduced by a factor two.

### 12.1.3 Advanced materials

In the design of the Renosaur the materials graphite and tungsten are used. Although these materials are becoming more usual for aircraft, the manufacturing techniques used in the processing of these materials are complicated and expensive.

# 13 COST ESTIMATION

This Section documents the Cost Estimation for the Renosaur. The procedures are based on the method outlined in Ref. 9 and the calculations are performed in AAA.

## 13.1 COST PHILOSOPHY

In the RFP the AIAA asks for a flyaway cost estimate for production runs of 1 and 10 units. The problem however, when producing a low production run, is that the price per aircraft is high. To get this price down to a reasonable value, the number of aircraft must grow. However, for the Reno Races, only one aircraft is necessary. To obtain a higher production run and thus a lower unit price, an additional market for the Renosaur is investigated. An attractive possibility is the military market for third-world countries. An aircraft that is currently flying in this market is the Pilatus PC-9M, which specifications are given in Table 13.1. The current unit price estimate for the Pilatus PC-9M is $ 6.2 million (Ref. 21).

**Table 13.1: Pilatus PC-9M (Ref. 21)**

| | |
|---|---|
| Takeoff Weight | 5,181 lbf |
| Empty Weight | 3,926 lbf |
| Length | 33.3 ft |
| Height | 3.26 ft |
| Wing Span | 33.4 ft |
| Wing Area | 175 $ft^2$ |
| Fuel Capacity | n/a |
| Range | 955 mi |
| Cruise Speed | 345 mph |
| Maximum Speed | 386 mph |
| Stall Speed | 89 mph |
| Climb Rate | 3,880 ft/min |
| Service Ceiling | 38,000 ft |
| Engine | P&W PT6A-62 |
| Power | 980 shp |

The Renosaur can achieve a better performance, including a top speed of 600 mph instead of 386 mph, for a lower price. The author believes it is feasible to sell the Renosaur to third-world countries and expand the production run. So far a number of 250 Pilatus PC-9 aircraft are built (Ref. 21). The author believes a production run of 1000 units is achievable. In this Section a flyaway cost estimate for a production run of 1 and 10 units, as specified by the AIAA, as well as 1000 units is presented.

## 13.2 COST ESCALATION FACTOR

The estimates for cost magnitudes in Ref. 9 are given for past year dollars. These costs are scaled from one year to another with the Cost Escalation Factor (CEF). The Cost Escalation Factor is based on the Consumer Price Index (CPI). CEF is calculated by taking a ratio of the CPI for "then year" and comparing it to the CPI of a base year. 1970 is used as a base year for the CEF.

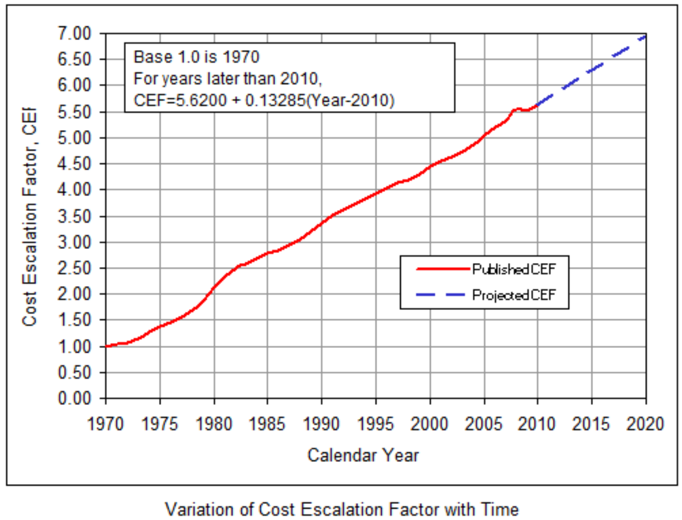


**Figure 14.2: Cost Escalation Factor**

Figure 13.2 shows the Cost Escalation Factor from 1970 to 2020. The AAA software determines the CEF in the calculations. The Cost Escalation Factor for the year 2011 is determined to be 5.75.

## 13.3 AMPR WEIGHT

The Aeronautical Manufacturers Planning Report (AMPR) Weight of the Renosaur is the basis for all cost calculations. The AMPR weight is determined with AAA. As can be seen in Figure 13.3, the AMPR Weight of the Renosaur is equal to 3161 lbf.

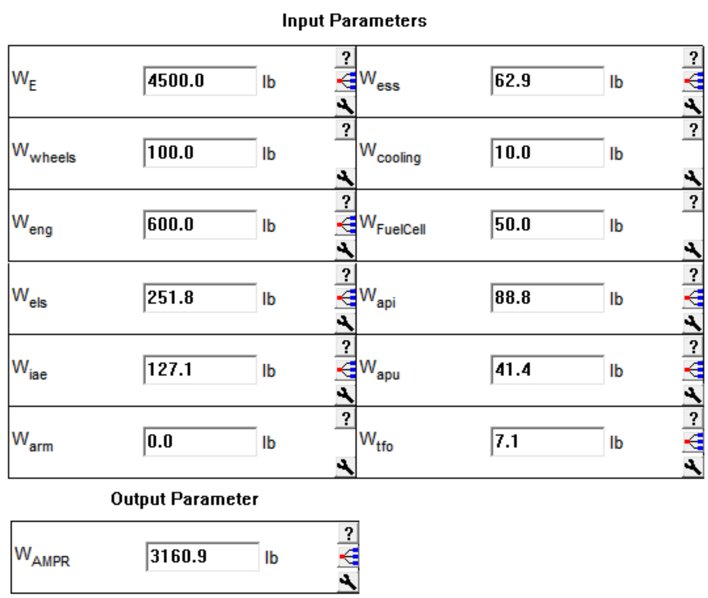


**Figure 13.3: AMPR Weight Determination in AAA**

## 13.4 RDTE COST

The RDTE Cost for the Renosaur is broken down into seven categories:

- Airframe Engineering and Design Cost, $C_{aed_r}$
- Development Support and Testing Cost, $C_{dst_r}$
- Flight Test Airplanes Cost, $C_{fta_r}$
- Flight Test Operations Cost, $C_{fto_r}$
- Test and Simulation Facilities Cost, $C_{tsf_r}$
- RDTE profit, $C_{pro_r}$
- Cost to finance the RDTE phases, $C_{fin_r}$

The RDTE cost is determined with AAA. Screenshots of this process can be found in Appendix B. The total RDTE cost for the Renosaur is as following:

$$C_{RDTE} = \$234{,}000{,}000$$

The RDTE cost is an initial cost that has to be made independent of the number of airplanes built. If the production run is expanded however, the RDTE cost per production airplane decreases rapidly. This is presented in Figure 13.4. The RDTE cost for a production run of 1000 airplanes is $ 0.23 million.

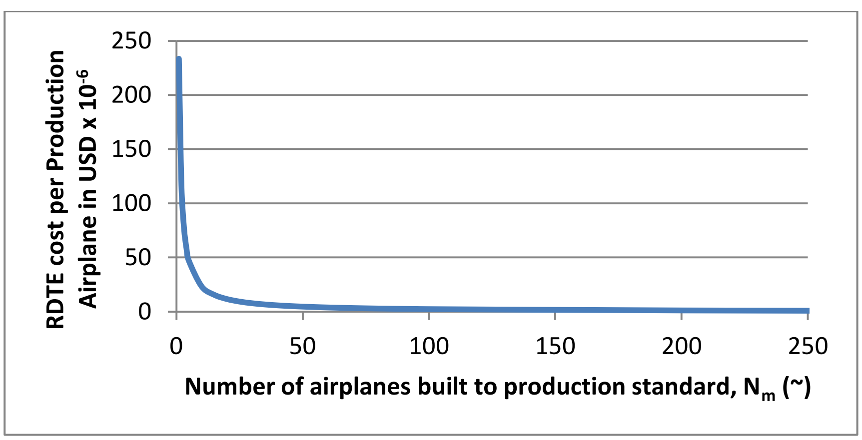


**Figure 13.4: Effect of Number of Airplanes built on the RDTE cost**

## 13.5 ACQUISITION COST

The total acquisition cost consists of the manufacturing cost of the aircraft plus the profit made by the manufacturer. The total airplane program manufacturing cost can be broken down into the following categories:

- Airframe Engineering and Design Cost, $C_{aed_m}$
- Airplane Production Cost, $C_{apc_m}$
- Production Flight Test Operations Cost, $C_{fto_m}$
- Cost of financing the manufacturing program, $C_{fin_m}$

Screenshots of the acquisition cost per category for the Renosaur can be seen in Appendix B. The total acquisition cost for a production run of 1 unit is presented in Figure 13.5.

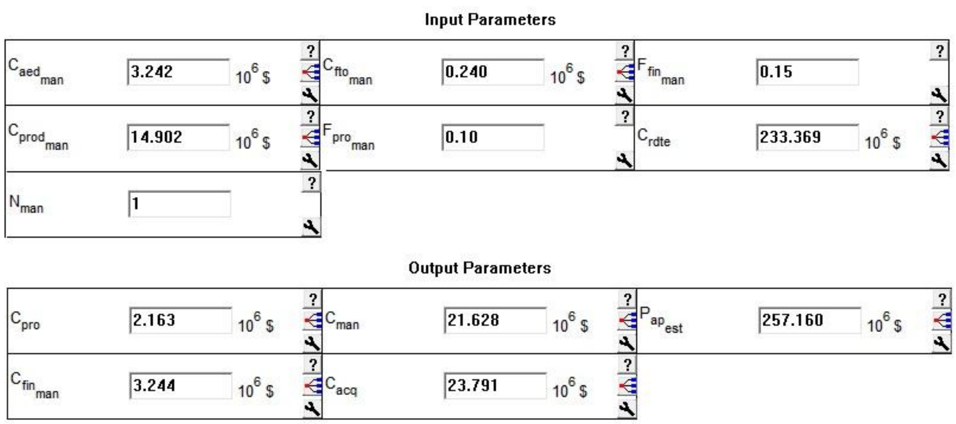


**Figure 13.5: Acquisition Cost for the Renosaur for a production run of 1 unit**

The airplane estimated price cost for the different production runs are as following:

- 1 unit: $ 257 million
- 10 units: $ 26.0 million
- 1000 units: $ 5.0 million

As can be seen, when a production run of 1000 units is achieved, the Renosaur will be a higher performance aircraft for a lower price than the Pilatus PC-9M.

## 13.6 OPERATING COST

The operating cost is assumed negligible for the production run of 1 and 10 units. However, if the Renosaur is sold to third-world countries for military use, the operating costs need to be taken into account. The operating cost for a military aircraft can be broken down in the following categories:

- Program Fuel, Oil and Lubricants Cost, $C_{POL}$
- Program Cost of Direct Personnel, $C_{PERSDIR}$
- Program Cost of Indirect Personnel, $C_{PERSIND}$
- Program Cost of Consumable Materials used in Conjunction with Maintenance, $C_{CONMAT}$
- Program Cost of Spares, $C_{SPARES}$
- Program Cost Associated with Depots, $C_{DEPOT}$
- Program Miscellaneous Cost, $C_{MISC}$

Screenshots of the acquisition cost per category for the Renosaur can be seen in Appendix B. The total acquisition cost for a production run of 1 unit is presented in Figure 13.6 and equals $20095 million or $5185/hr.

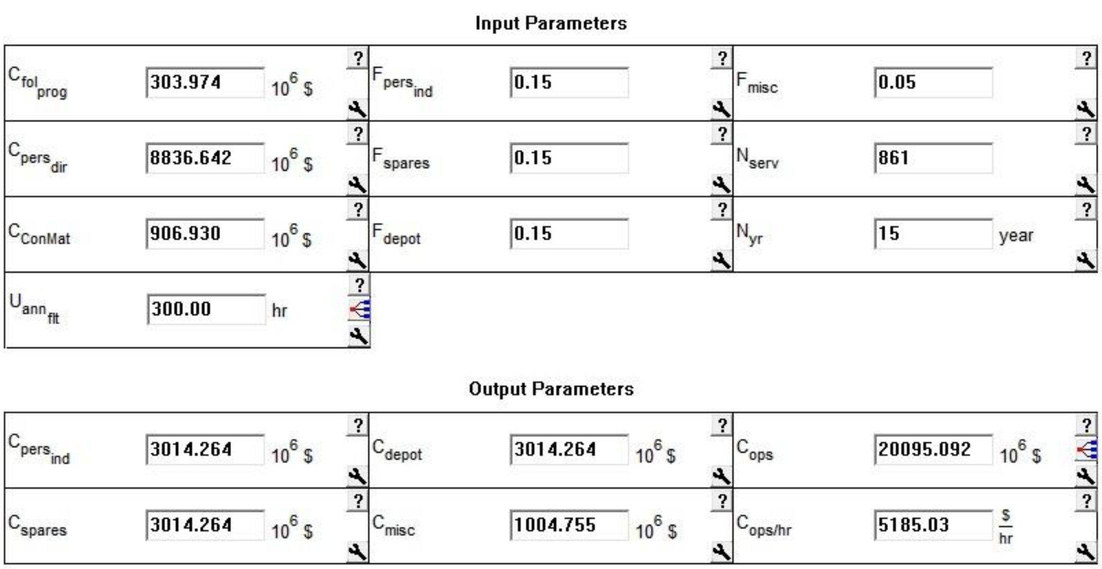


**Figure 13.6: Operating Cost for the Renosaur**

## 13.7 LIFE CYCLE COST AND DISPOSAL COST

The total life cycle cost for the 1000 units production run consists of the sum of the RDTE, acquisition and operation cost. A disposal factor of 0.01 is taken into account. The total lifecycle cost of the Renosaur equals $ 25380 million, as can be seen in Figure 13.7.

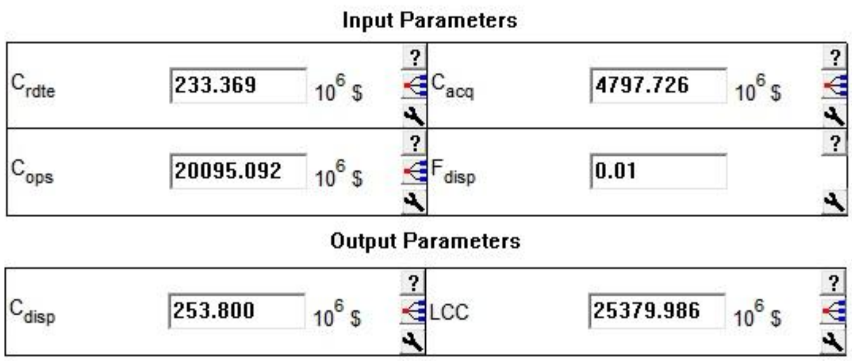


**Figure 13.7: Life Cycle and Disposal Cost for the Renosaur**

# 14 REFERENCES

1. Anon., “2006-2007 AIAA Undergraduate Team Aircraft Design Competition,” *American Institute of Aeronautics and Astronautics, AIAA Web Site* [http://www.aiaa.org/pdf/student/2011-2012-Ugrad-Ind-Aircraft-RFP.pdf] American Institute of Aeronautics and Astronautics, Lawrence, Kansas 66045, 20 October 2011, 2.44 am.
2. Anon., “National Championship Air Races”, Reno Air Racing Association Web Site [http://reports.airrace.org/] 11 December 2011, 3:59 pm.
3. Anon., “Race Course Information,” Reno Tahoe Web Site [http://www.visitrenotahoe.com/events/airrace/course] 08 December 2011, 1:14 pm.
4. Roskam, J., *Airplane Design Part I: Preliminary Sizing of Airplanes*, 4th edition, DARCorporation, Lawrence, Kansas, 2005.
5. Roskam, J., *Airplane Design Part II: Preliminary Configuration Design and Integration of the Propulsion System,* 4th edition, DARCorporation, Lawrence, Kansas, 2005.
6. Roskam, J., *Airplane Design Part III: Layout Design of Cockpit, Fuselage, Wing and Empennage: Cutaways and Inboard Profiles,* 4th edition, DARCorporation, Lawrence, Kansas, 2011.
7. Roskam, J., *Airplane Design Part IV: Layout of Landing Gear and Systems*, 6th edition, DARCorporation, Lawrence, Kansas, 2010.
8. Roskam, J., *Airplane Design Part V: Component Weight Estimation*, 3rd edition, DARCorporation, Lawrence, Kansas, 2003.
9. Roskam, J., *Airplane Design Part VIII: Airplane Cost Estimation: Design, Development, Manufacturing and Operating,* 3rd edition, DARCorporation, Lawrence, Kansas, 2006.
10. Anon., “Advanced Aircraft Analysis Software,” Design Analyze Research Corporation, Lawrence, Kansas, 2011.
11. Anon., “Shark FX Software,” PunchCAD, Minneapolis, Minnesota, 2011.
12. Morrison, W.D. Jr., “Advanced Airfoil Design Empirically Bases Transonic Aircraft-Drag Buildup Technique,” Lockheed-California Company, Burbank, California, January 1976.
13. Green, W., *War Planes of the Second World War: Fighters,* 1st edition, Vol. 4, Doubleday & Company, Inc., New York, 1973, pp. 4-12, 15-18, 47-59, 82-84, 88-96, 106-121, 136-152, 169-183.
14. Anon., *Jane’s All the World’s Aircraft 1992-1993,* 1st edition, Jane’s Information Group, London, pp. 439.

15. Anon., “Warbird Alley’s Aircraft Information, Histories, Links and More”, Warbird Alley, Warbird Alley Web Site [http://warbirdalley.com/acft.htm] 4 September 2011, 4:12 pm.
16. Anon., “Picture of the Week”, AAFO Web Site [http://www.aafo.com/gallery/07-23-01.htm], 11 September 2011, 3:59 pm.
17. Anon., “Strega Technical Specs & Drawings,” Team Strega Racing Enterprises, Team Strega Web Site [http://www.strega.com/#] 11 September 2011, 4:16 pm.
18. Anon., “Race 57 LLC 's Goodyear F2G-1D "Super" Corsair,” Warbird Depot Web Site [http://www.warbirddepot.com/], 11 September 2011, 4:10 pm.
19. Anon., “BMW F1 Engine Comparison,” MWERS Web Site [www.mwerks.com] MWERKS, 16 October 2011, 3:12 am.
20. Anon., “Garrett TPE331,” The Canadian Museum of Flight Web Site [http://www.canadianflight.org/content/garrett-tpe331] The Canadian Museum of Flight, 23 October 2011, 4:21 pm.
21. Anon., “PC-9M,” Pilatus Aircraft Web Site [http://www.pilatus-aircraft.com/#42] Pilatus Aircraft, Stans, Switzerland, 08 December 2011, 10:21 pm.